Extraordinary genome instability and widespread chromosome rearrangements during vegetative growth

Mareike Möller[1,2], Michael Habig[1,2], Michael Freitag[3], Eva H. Stukenbrock[1,2]

[1]Environmental Genomics, Christian-Albrechts University, Am Botanischen Garten 1-9, D-24118 Kiel, Germany

[2]Max Planck Institute for Evolutionary Biology, August-Thienemann-Str. 2, D-24306 Plön, Germany

[3]Department of Biochemistry and Biophysics, Oregon State University, Corvallis, OR 97331-7305, United States of America

Abstract

The haploid genome of the pathogenic fungus *Zymoseptoria tritici* is contained on "core" and "accessory" chromosomes. While 13 core chromosomes are found in all strains, as many as eight accessory chromosomes show presence/absence variation and rearrangements among field isolates. We investigated chromosome stability using experimental evolution, karyotyping and genome sequencing. We report extremely high and variable rates of accessory chromosome loss during mitotic propagation *in vitro* and *in planta*. Spontaneous chromosome loss was observed in 2 to >50 % of cells during four weeks of incubation. Similar rates of chromosome loss in the closely related *Z. ardabiliae* suggest that this extreme chromosome dynamic is a conserved phenomenon in the genus. Elevating the incubation temperature greatly increases instability of accessory and even core chromosomes, causing severe rearrangements involving telomere fusion and chromosome breakage. Chromosome losses do not impact the fitness of *Z. tritici in vitro*, but some lead to increased virulence suggesting an adaptive role of this extraordinary chromosome instability.

31 **Introduction**

32 Pathogenic fungi pose global threats to agriculture, human, and animal health. Pathogens
33 infecting plants and animals have been shown to rapidly adapt to changing environments,
34 including industrial agriculture and medical treatments, usually in response to adaptive
35 pressure caused by the widespread use of fungicides and pharmaceuticals (Selmecki et al.
36 2010; Bennett et al. 2014). The genomes of many prominent fungal plant pathogens exhibit
37 high levels of structural variation including isolate- or lineage-specific regions often
38 characterized by high repeat contents, and accessory chromosomes varying in frequency
39 among individual isolates (De Jonge et al. 2013; Persoons et al. 2014; Plissonneau &
40 Stürchler 2016). Structural variation is often associated with meiotic recombination, but
41 highly variable regions are also found in asexually and mostly asexually reproducing species
42 (Faino et al. 2016; Chuma et al. 2011; Wang et al. 2006). In several plant pathogenic fungi,
43 determinants of virulence, so called effector proteins, are located in dynamic regions of the
44 genome (Coleman et al. 2009; Ma et al. 2010; V. Miao et al. 1991). Accessory chromosomes
45 often carry genes that encode virulence determinants and are linked to pathogenicity.
46 Therefore, the absence of a particular chromosome in some species results in avirulent
47 phenotypes (Tsuge et al. 2016; Vlaardingerbroek et al. 2016; Ma et al. 2010; van Dam et al.
48 2018). Little is known about the mechanisms that drive the dynamics of accessory
49 chromosomes and highly variable regions in genomes of eukaryotic pathogens.

50 The plant pathogenic fungus *Zymoseptoria tritici* causes disease on wheat, especially in
51 Northern Europe and North America, resulting in extensive annual yield loss (Fones & Gurr
52 2015; Torriani et al. 2015). The *Z. tritici* reference isolate IPO323 contains eight accessory
53 chromosomes with sizes ranging from 0.4 to 1 Mb, accounting for 12% of the entire genome
54 (Goodwin, Ben M'Barek, et al. 2011). Chromosome rearrangements, including complete loss

55 of accessory chromosomes, are a frequent phenomenon in this fungus and have been widely
56 studied as a consequence of meiosis (Wittenberg et al. 2009; Croll et al. 2015; Fouche et al.
57 2017). Infection experiments with *Z. tritici* strains in which single or multiple accessory
58 chromosomes had been deleted showed that at least some accessory chromosomes encode
59 virulence factors that determine host specificity (Habig et al. 2017). In contrast to the core
60 chromosomes, accessory chromosomes are enriched with transposable elements and have
61 low gene density (Goodwin, M'barek, et al. 2011). Chromatin of accessory chromosomes
62 shows hallmarks of constitutive and facultative heterochromatin, consistent with the
63 observed transcriptional silencing of genes present on these chromosomes (Schotanus et al.
64 2015; Kellner et al. 2014; Rudd et al. 2015). The centromeres, subtelomeric regions and
65 telomeric repeats of accessory chromosomes are indistinguishable from those of core
66 chromosomes (Schotanus et al. 2015), suggesting that accessory chromosomes contain all
67 the required regions for proper chromosome segregation. The unusual high number of
68 accessory chromosomes, in combination with the extreme variability in chromosome
69 content among field isolates or progeny from controlled crosses, make *Z. tritici* an excellent
70 eukaryotic model to study accessory chromosomes and their dynamics (Mehrabi et al. 2007;
71 Stukenbrock et al. 2010; Goodwin, M'barek, et al. 2011; Wittenberg et al. 2009). Here, we
72 provide evidence for unexpectedly high rates of chromosome loss and changes during
73 asexual propagation, both *in vitro* and *in planta*. We describe the types of structural
74 rearrangements and overall variation in chromosome stability in this important crop
75 pathogen.

76 ## Results

77 **Accessory chromosomes are lost at a very high rate *in vitro***

78 To assess the stability of accessory chromosomes in *Z. tritici* we conducted an *in vitro* long-
79 term growth experiment. We used the *Z. tritici* isolate IPO323Δchr18, derived from the
80 reference strain IPO323 for which there is a completely assembled genome (Goodwin,
81 M'barek, et al. 2011). IPO323Δchr18 lost chromosome 18 during previous *in vitro*
82 propagation, and is here referred to as Zt09 (Kellner et al. 2014).

83 We propagated fungal cells in liquid culture at 18°C, including eight transfers to fresh
84 medium. After four weeks (representing ~80 cell divisions per cell), 576 single strains
85 originating from three replicate cultures were tested for the presence of the seven accessory
86 chromosomes from the Zt09 progenitor by a PCR assay. The presence of marker regions,
87 located close to the centromere, and the right and left telomere repeats of each accessory
88 chromosome, were tested (Table S1). When the screening by PCR suggested absence of an
89 accessory chromosome, we further validated the result by electrophoretic separation of the
90 fungal chromosomes by pulsed field gel electrophoresis (PFGE) (Figure 1 A and B). Thirty
91 eight of the 576 (~7 %) tested strains lacked one accessory chromosome. We did not find
92 strains that lacked more than one chromosome, but observe a clear trend where accessory
93 chromosomes 14, 15 and 16 were lost more frequently than smaller accessory
94 chromosomes (Table 1). For example, chromosome 14 was absent in eighteen strains,
95 chromosome 15 in eight and 16 in nine strains. The small chromosomes 20 and 21 were lost
96 only in two and one strain, respectively, whereas chromosomes 17 and 19 were never
97 absent following the *in vitro* propagation (Table 1 and Table S2).

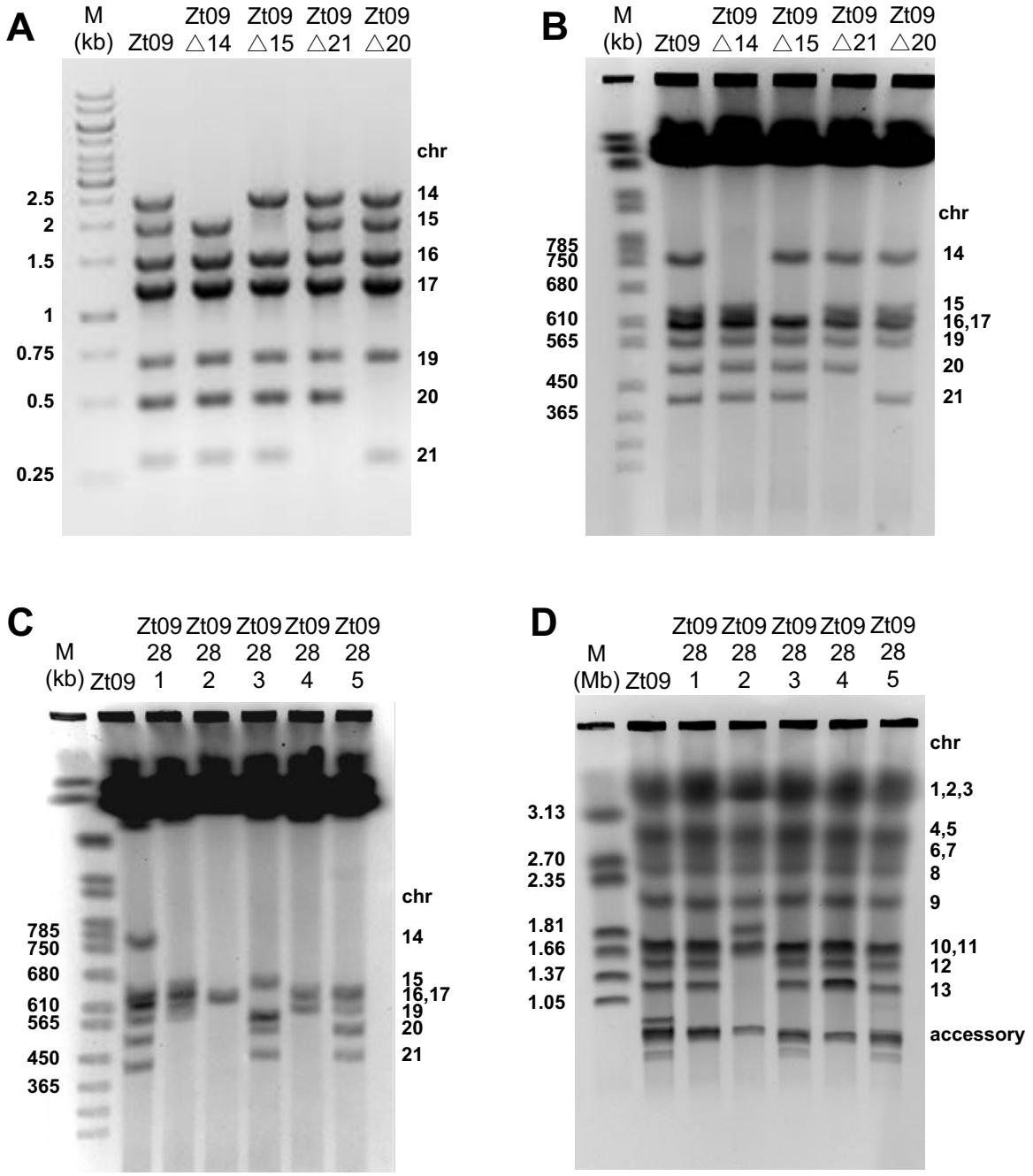

Figure 1: Screening by PCR and pulsed-field gel electrophoresis to identify accessory chromosome-loss strains in *Z. tritici*. (A) Screening by PCR of the progenitor Zt09 strain and evolved strains to assess chromosome losses using primer pairs located close to the centromeric region of the respective accessory chromosome. Multiplex PCR was used to simultaneously screen for the presence or absence of all accessory chromosomes in one strain. Absence of a PCR product indicates the absence of the chromosome; chromosome 18 is not present in Zt09. (B) Pulsed-field gel electrophoresis (PFGE) was conducted to validate the absence of accessory chromosomes in chromosome loss candidates identified by the initial PCR. Here, the separation of small accessory chromosomes of the progenitor strain Zt09 and four chromosome-loss strains is shown. The corresponding chromosome to each

band is indicated on the right. The absence of chromosomal bands confirms the loss of the respective chromosome; chromosome 18 is similar in length to 16 and 17 but is absent in Zt09. PFGE of the accessory (C) and mid-size (D) chromosomes of strains originating from the *in vitro* temperature stress experiment confirms multiple accessory chromosome losses, size alterations and chromosome fusions (see also Figures 3 and S1 and Table S3). The bands for chromosomes 3, 12, 13 and 21 are absent in strain 28-2, however, genome sequencing confirms that the chromosomes are still present in the genome (Figure 2C). The absence of bands on the PFGE can be explained by chromosome size changes whereby chromosomes 3 and 13 and 12 and 21 have experienced chromosome fusions (Figure 3 and S1). Note a new chromosome band with a size of ~1.8 Mb resulting from the fusion of chromosomes 12 and 21. In the strain 28-3, the accessory chromosomes 17 and 19 are shorter than the reference chromosomes due to chromosome breakage (Figure 2C and Table S3). Strain 28-4 has an additional band of ~1.2 Mb, representing the fusion of a duplicated chromosome 17 (Figure S1). All images of stained gels are color-inverted to make differences more obvious.

Table 1: Summary of chromosome losses in *Z. tritici* during evolution experiments *in vitro* and *in planta*. Listed are the number of cells that lost an accessory chromosome and which accessory chromosomes were lost. Sizes of the accessory chromosomes are listed next to the chromosome number. Strains with more than one chromosome lost are listed in brackets.

Chromosome (kb)	**Zt09 *in vitro* culture**	**Zt09 *in vitro* plate**	**IPO323 *in planta***	**Zt09 *in vitro* temperature stress**
14 (773)	18	0	1	108 (33)
15 (639)	8	0	6	2 (8)
16 (607)	9	4	1	0 (9)
17 (584)	0	0	0	0
18 (574)	N/A	N/A	7	N/A
19 (550)	0	0	2	2 (2)
20 (472)	2	0	0	1 (17)
21 (409)	1	1	0	1 (7)
Total chr loss strains	**38**	**5**	**17**	**114 (34)**
Total strains tested	**576**	**40**	**986**	**188**

132 We considered the possibility that natural selection acted on a large population of cells in
133 the liquid *Z. tritici* cultures and thereby contributed to the observed non-random
134 chromosome losses. To test this, we designed a second evolution experiment to propagate
135 individual cell lineages in the absence of selection. For this experiment, 40 strains originating
136 from one common progenitor (Zt09) were cultivated on plates. Every week, randomly
137 selected colonies derived from single cells were transferred to a fresh plate. These repeated
138 strong bottlenecks allowed us to propagate single lineages of *Z. tritici* without an effect of
139 natural selection (Barrick & Lenski 2013). After four weeks of growth (including four
140 transfers to new plates), the 40 evolved strains were tested for the presence of accessory
141 chromosomes as described above. Five out of 40 (~13 %) strains, twice as many as in the
142 previous experiment, lacked an accessory chromosome suggesting that selection in a larger
143 population of cells indeed had removed some of the spontaneously occurring chromosome
144 losses. Interestingly, in this experiment we observe the loss of only two different
145 chromosomes: Chromosome 16 was lost in four strains, and chromosome 21 in one strain.
146 Our two *in vitro* experiments suggest that chromosome loss is not entirely random, and that
147 specific chromosomes are lost at a higher rate (Table 1), depending on the *in vitro* growth
148 conditions. The frequency of chromosome losses during asexual growth *in vitro* is extremely
149 high in *Z. tritici* and exceeds previously reported spontaneous chromosome losses in *F.*
150 *oxysporum* f. sp. *lycopersici* by far (Vlaardingerbroek et al. 2016).
151
152 **Accessory chromosomes are unstable *in planta***
153 The growth of *Z. tritici* in rich medium *in vitro* is highly distinct from growth of the fungus in
154 its natural environment. *Zymoseptoria tritici* is a hemi-biotrophic pathogen infecting the
155 mesophyll of wheat leaves (Goodwin, M'barek, et al. 2011; Ponomarenko et al. 2011), where

156 it forms asexual fruiting bodies, pycnidia, containing presumably clonal conidiospores
157 (pycnidiospores). Pycnidia develop in the sub-stomatal cavities, where the environment and
158 nutrient availability differ from our tested *in vitro* conditions (Haueisen et al. 2017; Rudd et
159 al. 2015). To test whether chromosome loss occurs only *in vitro* or also during the natural
160 lifecycle of *Z. tritici*, we assessed the loss of accessory chromosomes *in planta*. We collected
161 pycnidia from wheat leaves infected with the *Z. tritici* strain IPO323 and tested single
162 pycnidiospores for the presence of accessory chromosomes. A total number of 968
163 pycnidiospores originating from 42 separate pycnidia were screened by PCR. In total, 17
164 strains missing an accessory chromosome were identified (~1.7%). Chromosomes 15 and 18
165 were the most frequently lost chromosomes, while chromosomes 17, 20 and 21 were not
166 lost in any of the strains (Table 1 and Table S2). As for the *in vitro* experiments, no strains
167 lacking more than one chromosome were found. Interestingly, chromosome 18, which was
168 found to be lost at high rates in our plant experiments, was shown to be frequently absent
169 in field isolates *of Z. tritici* (Croll et al. 2013; McDonald et al. 2016). In summary, our findings
170 show that chromosome loss in *Z. tritici* not only results from the non-disjunction of
171 homologous chromosomes during meiosis II, as proposed previously (Wittenberg et al.
172 2009), but also from frequent chromosome losses during asexual growth and mitotic spore
173 formation *in planta*. The observed frequency of chromosome losses *in planta* is not as high
174 as during *in vitro* growth, however, the number of mitotic divisions to develop pycnidia is
175 presumably lower than during four weeks of *in vitro* growth. Therefore, we propose that the
176 reduced number of chromosome losses *in planta* rather reflects the reduced number of cell
177 divisions than possible fitness effects of chromosome losses.
178
179

180 **Chromosome instability is greatly increased during exposure to heat stress**

181 In their natural environments, pathogens are exposed to various kinds of biotic and abiotic
182 stresses. For example, the local environment on the leaf surface can fluctuate severely in
183 temperature and humidity conditions (Zhan & McDonald 2011). We assessed the impact of
184 an increase in temperature on chromosome stability of *Z. tritici*. To this end, we cultivated
185 Zt09 *in vitro* at elevated temperatures, namely an increase of ten degrees Celsius from 18° to
186 28°C during four weeks of incubation. Subsequent screening by PCR for accessory
187 chromosomes revealed severe chromosome losses in the tested strains. Out of 188 evolved
188 and tested strains, 148 (~80 %) were missing at least one accessory chromosome.
189 Chromosome 14 was the most frequently lost chromosome and 34 evolved strains were
190 lacking more than one chromosome. The maximum number of missing chromosomes was
191 six in one strain (Table 1 and Table S2). PFGE revealed that karyotype alterations were not
192 restricted to simple chromosome loss as observed in the *in vitro* experiments at 18°C and
193 the *in planta* experiments. In contrast, we observed frequent size variation of both core and
194 accessory chromosomes as a consequence of chromosome breakage, fusions and
195 duplications (see below) (Figure 1C and 1D, Figure S1, Table S3).

196

197 **Genome sequencing of chromosome-loss strains reveals chromosome breakage and**
198 **fusion, but a low number of SNPs**

199 In total, we sequenced 19 genomes originating from the different *in vitro* and the *in planta*
200 experiment and the respective progenitor strains; all sequencing results have been
201 deposited in the Sequence Read Archive (SRA) under BioProject ID PRJNA428438. Overall,
202 we confirmed the absence of complete accessory chromosomes (Figure 2A), and we found
203 very few additional changes. After filtering to exclude reads of poor quality and coverage

204 (see Materials and Methods, Supplementary Text) we identified a total number of nine SNPs
205 in eight sequenced strains originating from the *in vitro* experiment in liquid culture at 18°C
206 and the *in planta* experiment. Of these, three SNPs were located in coding regions (Table
207 S4). Besides the complete loss of accessory chromosomes and the identified SNPs, we found
208 no other mutations when comparing the progenitor and evolved strains. However, we
209 identified SNPs distinguishing Zt09 from our IPO323 reference strain, and the published
210 genome sequence; most of these SNPs were in non-coding sequences (Table S4). As we
211 show chromosome losses in different strains, we conclude that the few point mutations do
212 not have measurable impact on chromosome loss.

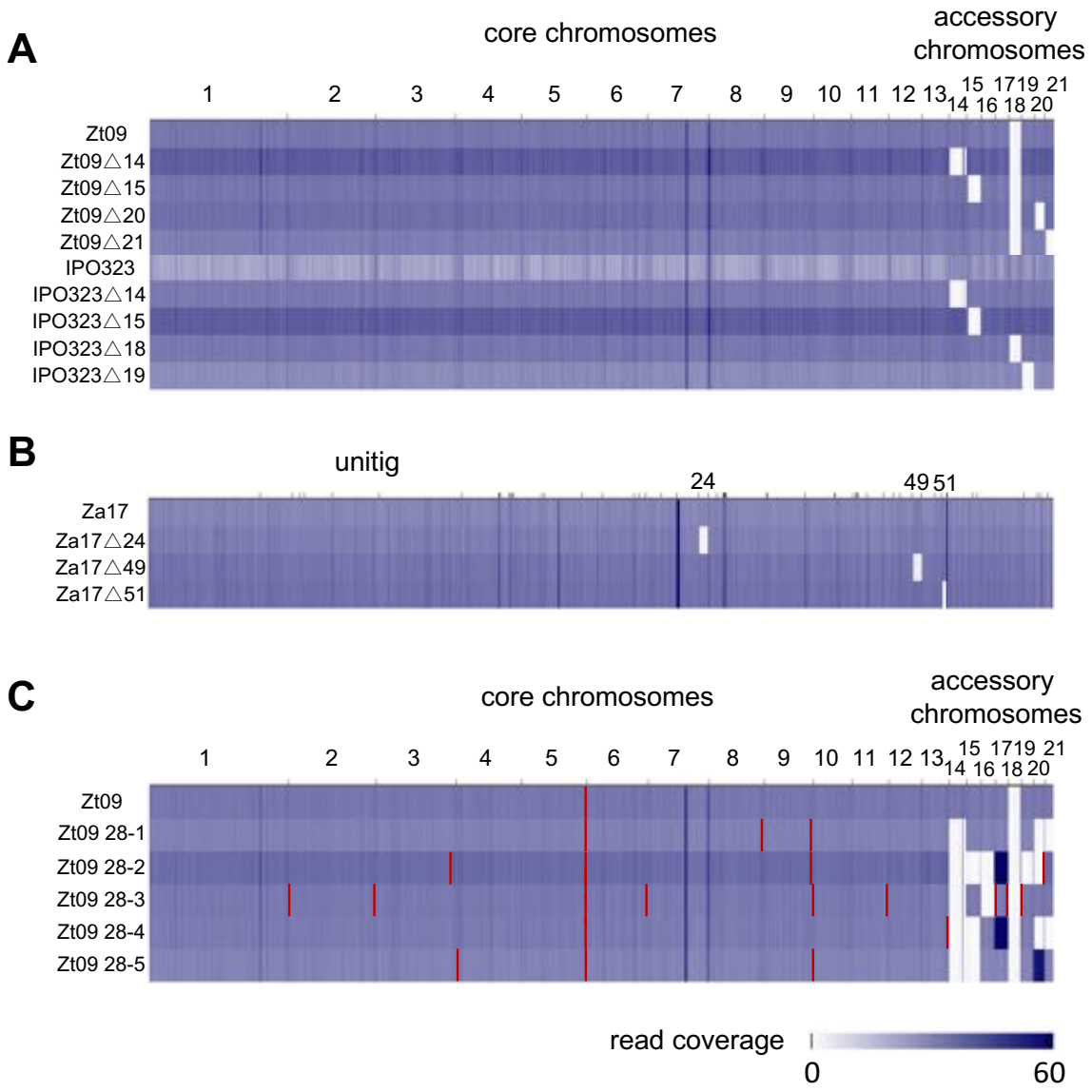

213

214 **Figure 2: Whole genome sequencing confirms loss of accessory chromosomes in *Z. tritici***
215 **and *Z. ardabiliae*.** The genomes of chromosome-loss strains derived from A) the *Z. tritici in*
216 *vitro* evolution experiment and the *in planta* pycnidiospore isolations, and B) the *Z.*
217 *ardabiliae in vitro* evolution experiment and the respective progenitor strains were
218 sequenced by paired-end Illumina sequencing and mapped to the respective reference
219 isolates, IPO323 (*Z. tritici*) or Za17 (*Z. ardabiliae*). The losses of entire chromosomes (white
220 boxes) were verified for each strain, but few mutations in form of SNPs, INDELs or copy
221 number variation were detected (Table S4). The *Z. tritici* reference genome consists of whole
222 chromosomes, while the *Z. ardabiliae* reference genome is composed of unitigs obtained
223 from the SMRT sequencing assembly (ordered by name of the unitig). C) Genome
224 sequencing of strains derived from the temperature stress experiment revealed, besides
225 verification of accessory chromosome losses, chromosome breaks at the ends of core and
226 accessory chromosomes (red lines) and accessory chromosome duplications. Darker blue
227 shading indicates higher coverage. Most repetitive sequences have a higher coverage than
228 single copy regions resulting in different shades of blue in the coverage graph. The intense
229 dark blue lines indicate high coverage regions on rDNA clusters or repetitive DNA due to
230 underestimation of repeats in the reference assembly (for example, the thin black line in
231 chromosome 7 indicates the location of several rDNA cluster repeats, the only such repeats
232 in the annotated genome sequence, but the expected true number of rDNA repeats is ~50).
233

234 Whole genome sequencing of five strains evolved at 28°C verified the losses of several
235 accessory chromosomes. Furthermore, comparison of the re-sequenced genomes of the
236 progenitor and the evolved strains revealed substantial size variation resulting from
237 chromosome breakage of core and accessory chromosomes, and duplications of accessory
238 chromosomes (Figure 2C). Chromosome breaks located close to the ends of chromosomes
239 resulted in shortened chromosomes caused by subtelomeric deletions of ~0.2-60 kb (Table
240 S3). Detailed analyses of the distribution of discordant paired-end reads mapping to
241 different chromosomes revealed a high number of reads at the chromosome breakpoints
242 with the respective read mates mapping to telomeric repeats (Figure 3). This suggested that
243 most chromosome breaks resulted in shorter chromosomes to which telomeres were added
244 *de novo*. Besides *de novo* telomere formation, we found evidence for fusion of core
245 chromosomes in strain Zt09 28-2, where discordant read mapping indicated fusion of the

246 right arms of chromosomes 3 and 13 (Table S3 and Figure 3). PFGE and Southern blots
247 further showed fusion of chromosomes 12 and 21 in Zt09 28-2 (Figure S1). In a previous
248 study, we reported evidence for the likely fusion of an ancestral accessory chromosome and
249 core chromosome 7 in the reference isolate IPO323 and Zt09 (Schotanus et al. 2015; Kellner
250 et al. 2014). Here, we deduced a fusion of the duplicated chromosome 17 in strain Zt09 28-4
251 (Figure 1C and D, Figure S1). Similar fusions of the same accessory chromosome 17 following
252 meiosis had been suggested previously, and "breakage-fusion bridge" cycles (McClintock
253 1938; McClintock 1941) were invoked as a mechanism to form a new accessory chromosome
254 (Croll et al. 2013). In total, in the five analyzed genomes derived from strains grown at 28°C,
255 we identified spontaneous changes: (1) fifteen chromosome breakages (twelve with *de novo*
256 telomere formation and three without evidence for new telomeres), (2) three chromosome
257 fusions, (3) three chromosome duplications, and (4) 16 chromosome losses (Table S3). A key
258 observation from our genome data analyses is the frequent involvement of *de novo*
259 telomere formation and chromosomal fusion as a mechanism to heal broken chromosome
260 ends. While this has been reported for cancer cells (Murnane 2012), it is generally
261 considered a rare event in normal, non-transformed cells. Here we show that *de novo*
262 telomere formation and chromosome fusion readily occur in a filamentous fungus during
263 growth at temperature stress.
264

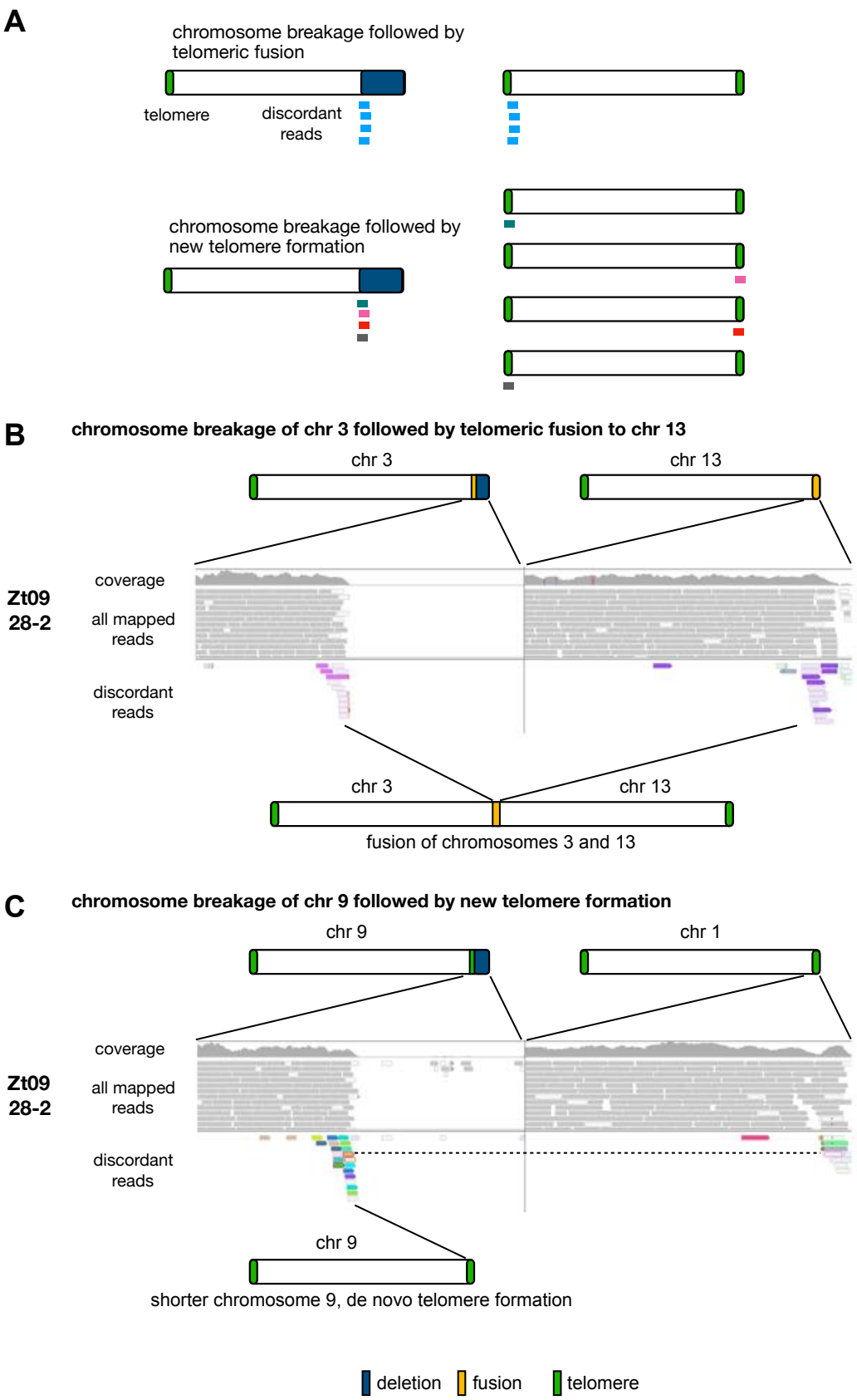

Figure 3: Discordant read analysis reveals chromosome fusion and chromosome breakage. A) Schematic illustration of discordant read mapping in the case of chromosome breakage and fusion. If chromosome breakage is followed by fusion to a different chromosome, the

269 discordantly mapping reads at the breakpoint will have their respective read mate on the
270 chromosome that is fused to the breakpoint. If breakage is followed by *de novo* telomere
271 formation, the discordant reads have their respective read mates on telomeric repeats on
272 random chromosomes. B and C) Read mapping to the genome of the reference isolate
273 IPO323. B) In the experimentally evolved strains of *Z. tritici* at 28°C, the fusion of
274 chromosomes 3 and 13 in the strain Zt09 28-2 is indicated by the increased occurrence of
275 discordant reads at the chromosome breakpoint of the right arm of chromosome 3 and the
276 right arm of chromosome 13. The color of the reads represents the chromosome their
277 respective mate is mapping to. Color intensity of the reads indicates the mapping quality. C)
278 New telomere formation at the breakpoint, here, as example, shown for chromosome 9 in
279 the strain Zt09 28-2. Telomere formation is indicated by a high number of discordant reads,
280 where the read mates are mapping to the telomeric repeats of different chromosomes. As
281 an example, the right telomere of chromosome 1 is shown, where one mate of the
282 discordant reads at the breakpoint of chromosome 9 is located (dashed line). A total of
283 twelve breakage events that were followed by *de novo* telomere formation were detected in
284 the five analyzed strains derived from the experiment at elevated temperature.
285

286 **Accessory chromosome instability also occurs in *Zymoseptoria* sister species**

287 To assess whether the high frequency of mitotic chromosome loss is specific to *Z. tritici*, we
288 conducted a short-term *in vitro* evolution experiment on the fungus *Z. ardabiliae,* a closely
289 related sister species of *Z. tritici* that infects wild grasses. We used the previously
290 characterized isolate STIR04 1.1.1 (Stukenbrock et al. 2011), here called Za17, in our
291 experiments.

292 We first generated a high-quality reference genome based on long-read SMRT sequencing
293 (Supplementary Text). To identify sequences of accessory chromosomes we first combined
294 analyses of a population genomic dataset and PFGE (Stukenbrock et al. 2011; Stukenbrock &
295 Dutheil 2018). Our analyses reveal at least four accessory chromosomes varying in their
296 frequency among 17 *Z. ardabiliae* isolates. Based on these, we designed primers to amplify
297 six loci located on putative accessory chromosomes of Za17 (Table S1).

298 Next, we conducted an *in vitro* evolution experiment at 18°C for four weeks in liquid culture
299 with Za17 as the progenitor strain. Screening of 288 single clones by PCR identified five

300 strains lacking one of the accessory chromosomes (~1.7%). We further verified the absence
301 of accessory chromosomes by PFGE and whole genome sequencing for three of the five *Z.*
302 *ardabiliae* strains (Figure 2B). These findings resemble the rapid loss of chromosomes in *Z.*
303 *tritici* and suggest a common phenomenon, most likely related to mitotic cell division in the
304 two *Zymoseptoria* species.
305
306 **Accessory chromosome losses affect *in planta* phenotypes**
307 We next addressed the impact of spontaneous chromosome loss by comparing the fitness of
308 the progenitor and evolved *Z. tritici* strains under different *in vitro* growth conditions, and
309 during infection of a susceptible wheat variety by comparing growth and pycnidia formation.
310 *In vitro*, the growth rate of strains lacking an additional accessory chromosome (Zt09Δ14 and
311 Zt09Δ21) was comparable to the growth rate of the progenitor, Zt09, but with a slight
312 tendency to slower growth of the derived chromosome-loss strains (Figure S2). For a more
313 detailed phenotypic characterization, we used the five chromosome-loss strains isolated
314 from pycnidia from the *in planta* experiment (Table S2). Several stress conditions including
315 osmotic, oxidative, temperature, and cell wall stresses were tested *in vitro.* We compared
316 the fungal phenotypes of the chromosome-loss strains and the progenitor strain IPO323 and
317 observed no difference in growth rate or colony morphology between any chromosome-loss
318 strain and IPO323 (Figure S3). *In planta*, however, we observed phenotypic differences
319 between the evolved chromosome-loss strains and their progenitor. We measured fitness by
320 counting the number of asexual fruiting bodies formed in stomata on infected wheat leaves
321 and found a slightly higher fitness of the chromosome-loss strains compared to the
322 progenitor strain (Figure 4). The difference was most pronounced for the strains lacking
323 chromosome 14 and chromosome 19 where the density of pycnidia was found to be

324 significantly higher (*p* values of 0.0003 and 0.015, Wilcoxon-Rank-Sum test and Holm's

325 correction for multiple testing) compared to the IPO323 progenitor (Figure 4).

326

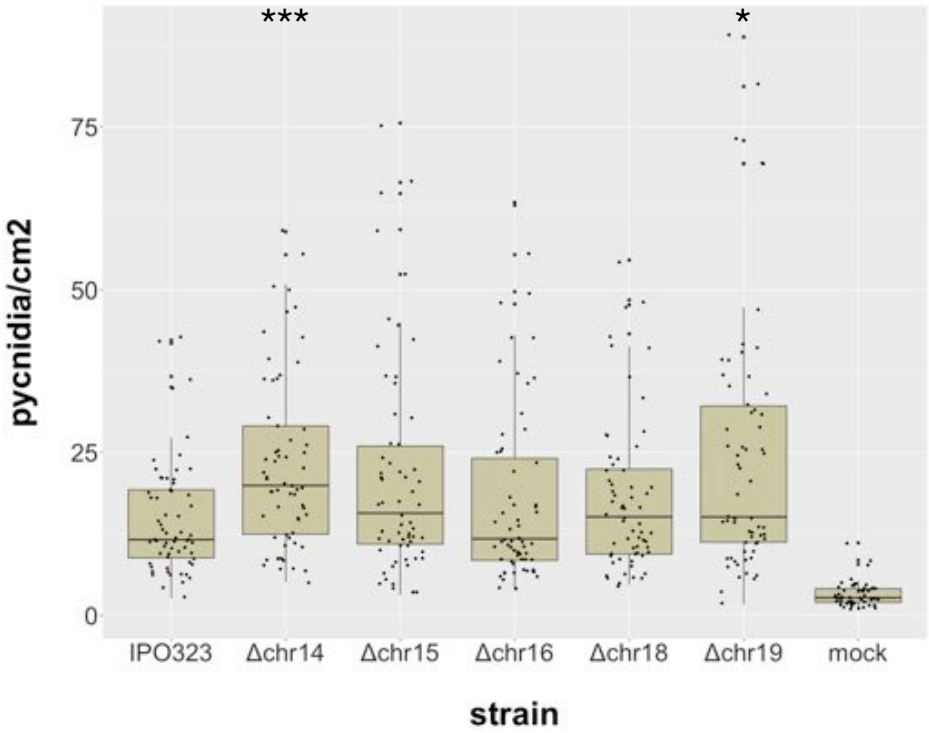

327

328 **Figure 4: *In planta* infection assays reveal a negative effect of accessory chromosomes on**
329 **fitness.** To investigate the effect of accessory chromosome losses on *Z. tritici* infection of
330 wheat, three independent experiments with the reference strain IPO323 and five
331 chromosome-loss strains were conducted. The fitness of each strain was measured by
332 counting the number of pycnidia per cm^2 on the leaf surface. Statistical analysis (Wilcoxon-
333 rank-sum test and Holms correction, p-values 0.0003 and 0.015) identified two
334 chromosome-loss strains (Chr. 14 and 19) that show a significantly higher number of
335 pycnidia compared to the reference strain IPO323 under the conditions used in this
336 experiment.

337

338

339 ## Discussion

340 **Consequences for evolution of accessory chromosomes**

341 Accessory chromosomes were proposed to serve as an 'evolutionary cradle' for creating
342 novel virulence genes without risking the disruption of essential genes on the core
343 chromosomes (Croll & McDonald 2012). Indeed, signatures for accelerated evolution were
344 shown by overall higher dN/dS ratios of genes on the accessory chromosomes compared to
345 the core chromosomes (Stukenbrock et al. 2010). However, natural selection acts at the
346 level of individuals and cannot maintain "a playground" for future beneficial effects. Rather,
347 we hypothesize that the dynamic of accessory chromosome loss reflects a dynamic in the
348 selective environment of *Z. tritici*, where under certain conditions these small chromosomes
349 confer a fitness advantage, while under different conditions they cause decrease in fitness. A
350 fitness advantage of chromosome-loss strains *in planta* may indicate the presence of
351 avirulence factors on at least some accessory chromosomes. Avirulence factors can be
352 recognized by the host to induce a resistance response resulting in reduction in virulence or
353 even abortion of infection (Petit-Houdenot & Fudal 2017; Zhong et al. 2017). Our previous
354 findings support this notion, as we found small but significant negative effects of accessory
355 chromosomes during host infection (Habig et al. 2017). In other pathogenic fungi, however,
356 the opposite effect has been demonstrated in several cases. A strong positive impact on
357 virulence of accessory chromosomes have been observed in *Fusarium oxysporum* f. spp. and
358 *Nectria haematococca* (Ma et al. 2010; Coleman et al. 2009; van Dam et al. 2018). In these
359 pathogens chromosome losses resulted in complete loss of pathogenicity. While these cases
360 are currently considered the norm, our observations show that responses to accessory
361 chromosome loss can be more varied. Even though this fungus is an important pathogen in
362 all wheat-growing countries, the biology of *Z. tritici* is still not completely understood.

363 Mating and overwintering in the soil or litter layer remain largely unknown lifecycle stages,
364 and we postulate that they impose different selection pressures on the fungus. During these
365 stages, accessory chromosomes may confer significant fitness advantages that have not
366 been demonstrated yet. Besides spontaneous chromosome loss during meiosis (Wittenberg
367 et al. 2009), accessory chromosomes have been shown to follow non-Mendelian segregation
368 and are transmitted at a significantly higher rate than expected, if one of the two mating
369 partners lacks an accessory chromosome (Habig et al, submitted). While there is no
370 comprehensive mechanistic explanation yet, chromosome conservation by re-replication
371 during meiosis may counteract the chromosome loss during vegetative growth and
372 therefore maintain accessory chromosomes in pathogen populations. In *Alternaria*
373 *alternata*, the spontaneous loss of a conditionally dispensable chromosome during sub-
374 culturing has been described for one isolate (Johnson et al. 2001). Furthermore, loss of a
375 conditionally dispensable chromosome after meiosis has been observed in *Nectria*
376 *haematococca* (aka *Fusarium solani* MPVI) (V. P. Miao et al. 1991). A recent study of the
377 plant pathogenic fungus *Fusarium oxysporum* forma specialis *lycopersici* describes the
378 spontaneous loss of dispensable chromosomes *in vitro* in one cell out of 35,000
379 (Vlaardingerbroek et al. 2016). This rate is much lower than the chromosome loss rate that
380 we observe in *Z. tritici* and *Z. ardabiliae*, where, depending on the growth conditions, more
381 than one cell out of two to one cell out of 50, lacks an accessory chromosome. In
382 combination, these results indicate that chromosome instability is a common phenomenon
383 in fungi, but the stability of chromosomes can vary substantially between different species.
384 Studies in *Saccharomyces* and *Candida* species have shown that chromosome loss resulting
385 in aneuploidy is a relatively frequent phenomenon in diploid cells and is advantageous under
386 certain conditions (Kumaran et al. 2013; Bennett et al. 2014; Selmecki et al. 2010; Zhu et al.

387 2014). The loss of chromosomes in haploid organisms, such as *Z. tritici*, is expected to have
388 more severe consequences, as genetic information is lost from the cell. We considered,
389 however, that the effect of rapid chromosome loss or instability may be advantageous if
390 these traits are selected for in pathogens like *Zymoseptoria*.
391 The temperature stress experiment *in vitro* showed that genome instability in *Z. tritici,* at
392 this temperature, is not restricted to the accessory chromosomes, but also involves the core
393 genome. New chromosome formation induced by telomere to telomere fusion followed by
394 breakage of the dicentric chromosome was reported in *Cryptococcus neoformans* (Fraser et
395 al. 2005) but likely occurred during meiosis rather than mitosis. In the asexual *Candida*
396 *glabrata*, clinical isolates frequently inhabit chromosomal rearrangements indicating that
397 structural variation acts as a virulence mechanism (Poláková et al. 2009) and might be a
398 response to stresses such as antifungal treatment or elevated temperature as observed
399 here. The instable regions close to the chromosome ends on the core chromosomes,
400 however, show structural characteristics similar to the accessory chromosomes, such as
401 higher repeat content, lower gene density and specific histone modification patterns
402 (Dhillon et al. 2014; Grandaubert et al. 2015; Schotanus et al. 2015).
403 The accessory chromosomes of *Z. tritici* do not differ in terms of centromere or telomere
404 organization from the core chromosomes, but the chromatin is largely transcriptionally
405 inactive and potentially more condensed due to an enrichment with the histone H3 that is
406 trimethylated at lysine 27 (H3K27me3), which covers almost all of the accessory
407 chromosomes (Schotanus et al. 2015). H3K27me3 is also enriched in subtelomeric regions of
408 core chromosomes, that we show here as prone to instability. High-resolution microscopic
409 analyses indicate an unusual localization of centromeres in the *Z. tritici* nuclei, suggesting a
410 distinct spatial organization of different chromosomes (Schotanus et al. 2015).

411 Heterochromatin has been found close to the nuclear periphery, and H3K27me3 has been
412 shown to be involved in facilitating lamina-proximal positioning (Harr et al. 2015). We
413 hypothesize that the heterochromatic structure reflects a distinct physical organization of
414 core and accessory chromosomes and likely the subtelomeric regions in the nucleus of *Z.*
415 *tritici*, and that this is correlated to the instability of heterochromatic regions and
416 chromosomes. A Hi-C study on *Neurospora crassa* showed that absence of H3K27me3
417 resulted in movement of subtelomeric regions and centromeres from the nuclear periphery
418 into the nuclear matrix (Klocko et al. 2016). Further experiments focusing on localization of
419 specific *Zymoseptoria* chromosomes in the nucleus by cytology or Hi-C (Galazka et al. 2016)
420 should be conducted to address this hypothesis.
421 In conclusion, using experimental evolution, electrophoretic karyotyping and genome
422 sequencing we showed that the accessory chromosomes of *Z. tritici* are highly unstable
423 during asexual growth across numerous mitotic cell divisions ("mitotic growth") *in vitro* as
424 well as *in planta.* Surprisingly, increasing the temperature from 18 to 28°C dramatically
425 increased overall genome instability in *Z. tritici*. Besides chromosome losses we observed
426 structural variation in form of chromosome breakage, duplication, and fusion involving both
427 core and accessory chromosomes, and all events were increased near telomeric sequences.
428 In *Z. tritici,* all of these chromosome abnormalities have thus far been associated with
429 meiosis (Croll et al. 2013; Wittenberg et al. 2009), however, our study highlights an
430 important role of mitotic growth in generating genetic diversity. The variability in
431 chromosome number and structure obtained over a relatively short period of time (during
432 one infection event, or four weeks of vegetative growth) correlates with the genomic
433 diversity observed in field populations of this important plant pathogen (Linde et al. 2002;
434 Mehrabi et al. 2007; Zhan et al. 2003; McDonald & Martinez 1991). Our findings

435 demonstrate that even sexual fungal pathogens can accelerate the generation of new
436 genetic diversity by mitosis-associated structural variation. The mitotic events responsible
437 for these rearrangements are still to be characterized.
438 Lastly, chromosome instability has been observed in various organisms and is a frequent
439 phenomenon in cancer cells (McGranahan et al. 2012). Epigenetic factors and
440 heterochromatin in particular have been shown to impact chromosome stability in human
441 cancer cells (Slee et al. 2012). The accessory chromosome dynamics correlating with distinct
442 chromatin patterns suggest that *Z. tritici* may provide a new model for mechanistic studies
443 of chromosome instability in cancer cells.

444 ## Materials and Methods

445 **Short term *in vitro* growth experiment in liquid culture**

446 *Zymoseptoria* strains were diluted from glycerol stocks (-80°C), plated on YMS agar (4 g yeast
447 extract, 4 g malt extract, 4 g sucrose, and 20 g agar per 1 liter) plates and grown for seven
448 days at 18°C to obtain single colonies. One single colony was picked and suspended in 100 µL
449 of YMS. Three replicate cultures were inoculated with 20 µL of cells from the single colony
450 (~50,000 cells). Cells were grown in 25 mL YMS medium at 18°C or 28°C shaking at 200 rpm
451 and 900 µL of the cultures were transferred to fresh medium after 3-4 days of growth. In
452 total eight transfers were conducted, for a total time course of four weeks.

453

454 **Short term *in vitro* growth experiment on agar plates**

455 A single colony derived directly from a plated dilution of frozen stock for Zt09 (IPO323Δ18)
456 was resuspended in 1000 µL YMS including 25% glycerol by 2 min vortexing on a VXR basic
457 Vibrax at 2,000 rpm, and 10-50 µL were replated onto a YMS agar plate. Forty replicates
458 were produced. Cells were grown for seven days at 18°C whereby a random colony (based
459 on vicinity to a prefixed position on the plate) derived from a single cell was picked and
460 transferred to a new plate as described above. The transfer was conducted for a total of four
461 times before a randomly chosen colony of each replicate was PCR screened and their
462 complement on accessory chromosomes characterized as described below.

463

464 **Screening by PCR**

465 Cells from transfer eight of liquid cultures were diluted and plated on YMS-agar plates to
466 obtain single colonies. To extract DNA, single colonies were suspended in 50 µL of 25 mM
467 NaOH and boiled at 98°C for 10 min; 50 µL of 40 mM Tris-HCl, pH 5.5, were added and 4 µL

468 were used as template for the PCR. Primers for the right and left subtelomeric regions and
469 close to the centromere were used for the chromosome loss screening in our *Z. tritici*
470 isolates, for *Z. ardabiliae* primers in the center of candidate accessory chromosome unitigs
471 were used. Primers and expected fragment lengths are listed in Table S1. Primers were
472 designed with Clonemanager (Sci-Ed Software, Denver, USA) and MacVector and ordered
473 from eurofins Genomics (Ebersberg, Germany).
474
475 **Plant experiments and pycnidia isolation**
476 Growth conditions for plants were 16 h at light intensity of ~200 µmol/$m^{-2}s^{-1}$ and 8 h
477 darkness in growth chambers at 20°C with 90% humidity. Seeds of the *Z. tritici* susceptible
478 wheat cultivar Obelisk (Wiersum Plantbreeding BV, Winschoten, The Netherlands) were
479 germinated on wet sterile Whatmann paper for four days at growth conditions before
480 potting. Following potting, plants were further grown for seven days before infection.
481 For the phenotypic analyses, three independent experiments were conducted and 21 plants
482 were used per strain per experiment. An ~5 cm long section on the second leaf of each plant
483 was infected by brushing a cell suspension with 10^7 cell/ml in H_2O + 0.1% Tween 20 on the
484 abaxial and adaxial side of the second leaf. Plants were placed into sealed bags containing
485 ~1 L of water for 48 h to facilitate infection at maximum air humidity. Infected leaf areas
486 were harvested 21 days post infection for further phenotypic analysis or prepared for
487 pycnidia isolation by surface sterilization with 1.2% NaClO for 2 min followed by 70% ethanol
488 for a few seconds and washed twice with H_2O. Leaves were placed into a sterile environment
489 with maximum air humidity and incubated for 7-14 days at plant growth conditions. Spores
490 that had been pressed out from pycnidia were isolated using a sterile syringe needle and
491 resuspended into 50 µL YMS medium with 50% glycerol. Cells were suspended by 30 min

492 vortexing on a VXR basic Vibrax (IKA, Staufen, Germany) at 2,000 rpm, plated on YMS agar,
493 and incubated for seven days at 18°C. Colonies arising from single cells were PCR screened
494 and their complement on accessory chromosomes characterized as described below.
495
496 **Phenotypic characterization of infected leaves**
497 Harvested leaves were taped to a sheet of paper and scanned using a flatbed scanner at a
498 resolution of 2,400 dpi. The scanned leaves were analyzed using ImageJ (Schneider et al.
499 2012) and a plug-in described previously (Stewart et al. 2016). The measurement of
500 pycnidia/cm^2 was used for further statistical analyses in R (Ihaka & Gentleman 1996). The
501 Wilcoxon-Rank-Sum test and the Holm's correction for multiple testing were applied to
502 assess statistical differences between the samples.
503
504 ***In vitro* phenotype assay**
505 A spore solution containing 10^7 cells/mL and tenfold dilution series to 1,000 cells/mL was
506 prepared. To test for responses to different stress conditions *in vitro*, YMS plates containing
507 NaCl (0.5 M and 1 M), sorbitol (1 M and 1.5 M), Congo Red (300 µg/mL and 500 µg/ml), H_2O_2
508 (1.5 mM and 2 mM), MMS (methyl methanesulfonate, 0.01 %), a H_2O-agar plate and two
509 plates containing only YMS were prepared. Three µL of the spore suspension dilutions were
510 pipetted on the plates and incubated at 18°C for seven days. One of the YMS plates was
511 incubated at 28°C to test for thermal stress responses.
512
513 ***In vitro* growth assay**
514 YMS liquid cultures containing 10^5 cells/mL of either Zt09 or the chromosome-loss strains
515 Zt09Δ14 and Zt09Δ21 were prepared. Three replicates per strain were used in each

516 experiment. The spores were grown for four days at 18°C at 200 rpm in 25 mL YMS and the
517 OD_{600} was measured at different time points throughout the experiment. The data was fitted
518 using the R package growthcurver (Sprouffske & Wagner 2016) and the r values of each
519 replicate used for statistical comparison. Wilcoxon rank-sum test was used to compare the r
520 values of the different strains.
521
522 **Pulsed field gel electrophoresis (PFGE) and Southern blotting**
523 Fungal strains were grown in YMS medium for five days. Cells were harvested by
524 centrifugation for 10 min at 3,500 rpm. 5 x 10^8 cells were used for plug preparation. The cells
525 were resuspended in 1 mL H_2O and mixed with 1 mL of 2.2 % low range ultra agarose (Bio-
526 Rad, Munich, Germany). The mixture was pipetted into plug casting molds and cooled for 1 h
527 at 4°C. The plugs were transferred to 50 mL screw cap Falcon tubes containing 5 mL of lysis
528 buffer (1 % SDS; 0.45 M EDTA; 1.5 mg/ml proteinase K, Roth, Karlsruhe, Germany), and
529 incubated in lysis buffer for 48 h at 55°C, replacing the buffer once after 24 h. Chromosomal
530 plugs were washed three times for 20 min with 1 x TE buffer before storage in 5 mL of 0.5 M
531 EDTA at 4°C. PFGE was performed with a CHEF-DR III pulsed field electrophoresis system
532 (BioRad, Munich, Germany). To separate the small accessory chromosomes, the following
533 settings were applied: switching time 50 s – 150 s, 5 V/cm, 120° angle, 1 % pulsed field
534 agarose (BioRad, Munich, Germany) in 0.5 x TBE (TRIS/borate/EDTA) for 48 h. Separation of
535 mid-size chromosomes was conducted with the settings: switching time 250 s – 1000 s, 3
536 V/cm, 106° angle, 1 % pulsed field agarose in 0.5 x TBE for 72 h. *Saccharomyces cerevisiae*
537 chromosomal DNA (BioRad, Munich, Germany) was used as size marker for the accessory
538 chromosomes, and *Hansenula wingei* chromosomal DNA (BioRad, Munich, Germany) for
539 mid-size chromosomes. Gels were stained in ethidium bromide staining solution (1 µg/ml

540 ethidium bromide in H_2O) for 30 min. Detection of chromosomal bands was performed with
541 the GelDocTM XR+ system (Bio-Rad, Munich, Germany).
542 Southern blotting was performed as described previously (Southern 1975) using DIG-labeled
543 probes generated with the PCR DIG labeling Mix (Roche, Mannheim, Germany) following the
544 manufacturer's instructions.
545
546 **Sequencing and genome comparison**
547 DNA for whole genome sequencing was prepared as described in (Allen et al. 2006). Library
548 preparation with a reduced number of PCR cycles (four cycles) and sequencing were
549 performed by the Max Planck Genome Center, Cologne, Germany
550 (http://mpgc.mpipz.mpg.de/home/) using an Illumina HiSeq3000 machine, obtaining ~30x
551 coverage with 150-nt paired-end reads. Raw reads were quality filtered using Trimmomatic
552 and mapped to the reference genome of *Z. tritici* or *Z. ardabiliae* using bowtie2. SNP calling
553 was conducted with samtools and bcftools and further quality filtered. The filtered SNPs
554 were validated by manual inspection. The data was visualized in IGV (Integrative Genomics
555 Viewer, http://software.broadinstitute.org/software/igv/) (Thorvaldsdóttir et al. 2013).
556 Detailed commands for each step of the data processing pipeline can be found in the
557 Supplementary Text.
558
559 **Accession numbers:** The sequencing data generated for this project were deposited in the
560 Sequence Read Archive under BioProject ID PRJNA428438.

Acknowledgements

Marcello Zala, Daniel Croll and Christoph J. Eschenbrenner are acknowledged for the preparation and assembly of the SMRT sequencing. Kathrin Happ for assistance during plant experiments. We thank all current and past members of the Environmental Genomics Group for fruitful discussions and overall support. Research in the group of EHS is supported by the Max-Planck Society, the state of Schleswig-Holstein and the DFG priority program SPP1819.

Competing interests

The authors declare no competing interests.

Author contributions

MM: Conceptualization, Investigation, Visualization, Formal analysis, Writing—original draft

MH: Conceptualization, Investigation (*in planta* chromosome loss), Writing—review & editing

MF: Conceptualization, Formal analysis, Writing—review & editing, Supervision

EHS: Conceptualization, Formal analysis, Writing—review & editing, Supervision, Project administration, Funding acquisition

578 **References**
579
580 Allen, G.C. et al., 2006. A modified protocol for rapid DNA isolation from plant tissues using
581 cetyltrimethylammonium bromide. *Nature protocols*, 1(5), pp.2320–2325.
582 Barrick, J.E. & Lenski, R.E., 2013. Genome dynamics during experimental evolution. *Nature*
583 *reviews. Genetics*, 14(12), pp.827–39.
584 Bennett, R.J., Forche, A. & Berman, J., 2014. Rapid mechanisms for generating genome
585 diversity: Whole ploidy shifts, aneuploidy, and loss of heterozygosity. *Cold Spring*
586 *Harbor Perspectives in Medicine*, 4(10).
587 Bolger, A.M., Lohse, M. & Usadel, B., 2014. Trimmomatic: A flexible trimmer for Illumina
588 sequence data. *Bioinformatics*, 30(15), pp.2114–2120.
589 Chin, C.-S. et al., 2013. Nonhybrid, finished microbial genome assemblies from long-read
590 SMRT sequencing data. *Nature Methods*, 10(6), pp.563–569.
591 Chuma, I. et al., 2011. Multiple Translocation of the *AVR-Pita* Effector Gene among
592 Chromosomes of the Rice Blast Fungus *Magnaporthe oryzae* and Related Species. *PLoS*
593 *Pathog*, 7(7), p.e1002147.
594 Coleman, J.J. et al., 2009. The genome of Nectria haematococca: Contribution of
595 supernumerary chromosomes to gene expansion. *PLoS Genetics*, 5(8).
596 Croll, D. et al., 2015. The impact of recombination hotspots on genome evolution of a fungal
597 plant pathogen. *Genetics*, 201(3), pp.1213–1228.
598 Croll, D. & McDonald, B.A., 2012. The accessory genome as a cradle for adaptive evolution in
599 pathogens. *PLoS Pathogens*, 8(4), pp.8–10.
600 Croll, D., Zala, M. & McDonald, B. a, 2013. Breakage-fusion-bridge cycles and large insertions
601 contribute to the rapid evolution of accessory chromosomes in a fungal pathogen. *PLoS*
602 *genetics*, 9(6), p.e1003567.
603 Crosthwaite, S.K., Dunlap, J.C. & Loros, J.J., 1997. Neurospora wc-1 and wc-2: transcription,
604 photoresponses, and the origins of circadian rhythmicity. *Science*, 276(5313), pp.763–
605 769.
606 van Dam, P. et al., 2018. Use of Comparative Genomics-Based Markers for Discrimination of
607 Host Specificity in Fusarium oxysporum. *Applied and Environmental Microbiology* ,
608 84(1).
609 Dhillon, B. et al., 2014. The landscape of transposable elements in the finished genome of
610 the fungal wheat pathogen Mycosphaerella graminicola. *BMC genomics*, 15(1), p.1132.
611 Faino, L. et al., 2016. Transposons passively and actively contribute to evolution of the two-
612 speed genome of a fungal pathogen. *Genome Research*, p.gr.204974.116.
613 Fones, H. & Gurr, S., 2015. The impact of Septoria tritici Blotch disease on wheat: An EU
614 perspective. *Fungal Genetics and Biology*, 79, pp.3–7.
615 Fouche, S. et al., 2017. Meiosis leads to pervasive segregation distortion and copy-number
616 variation in accessory chromosomes of the wheat pathogen Zymoseptoria tritici;
617 *bioRxiv*. Available at: http://biorxiv.org/content/early/2017/11/07/214882
618 Fraser, J.A. et al., 2005. Chromosomal Translocation and Segmental Duplication in
619 Cryptococcus neoformans Chromosomal Translocation and Segmental Duplication in
620 Cryptococcus neoformans. Eukaryotic Cell , 4(2), pp.401–406.
621 Galazka, J.M. et al., 2016. *Neurospora* chromosomes are organized by blocs of importin
622 alpha- dependent heterochromatin that are largely independent of H3K9me3. *Genome*
623 *Research*, (541), pp.1069–1080.
624 Goodwin, S.B., M'barek, S. Ben, et al., 2011. Finished genome of the fungal wheat pathogen
625 Mycosphaerella graminicola reveals dispensome structure, chromosome plasticity, and

626 stealth pathogenesis. *PLoS genetics*, 7(6), p.e1002070.
627 Grandaubert, J., Bhattacharyya, A. & Stukenbrock, E.H., 2015. RNA-seq Based Gene
628 Annotation and Comparative Genomics of Four Fungal Grass Pathogens in the Genus
629 Zymoseptoria Identify Novel Orphan Genes and Species-Specific Invasions of
630 Transposable Elements. *G3 (Bethesda, Md.)*, 5(July), p.g3.115.017731-.
631 Habig, M., Quade, J. & Stukenbrock, E.H., 2017. Forward genetics approach reveals host-
632 genotype dependent importance of accessory chromosomes in the fungal wheat
633 pathogen Zymoseptoria tritici. *mBio*, 8(6), p.Forthcoming.
634 Harr, J.C. et al., 2015. Directed targeting of chromatin to the nuclear lamina is mediated by
635 chromatin state and A-type lamins. *Journal of Cell Biology*, 208(1), pp.33–52.
636 Haueisen, J. et al., 2017. Extremely flexible infection programs in a fungal plant pathogen.
637 *bioRxiv*, 49(0), p.229997. Available at:
638 https://www.biorxiv.org/content/early/2017/12/06/229997.
639 Ihaka, R. & Gentleman, R., 1996. R: A Language for Data Analysis and Graphics. *Journal of*
640 *Computational and Graphical Statistics*, 5(3), pp.299–314.
641 Johnson, L.J. et al., 2001. Spontaneous loss of a conditionally dispensable chromosome from
642 the Alternaria alternata apple pathotype leads to loss of toxin production and
643 pathogenicity. *Current Genetics*, 40(1), pp.65–72.
644 De Jonge, R. et al., 2013. Extensive chromosomal reshuffling drives evolution of virulence in
645 an asexual pathogen. *Genome Research*, 23(8), pp.1271–1282.
646 Kellner, R. et al., 2014. Expression Profiling of the Wheat Pathogen Zymoseptoria tritici
647 Reveals Genomic Patterns of Transcription and Host-Specific Regulatory Programs.
648 *Genome biology and evolution*, 6(6), pp.1353–65.
649 Klocko, A.D. et al., 2016. Normal chromosome conformation depends on subtelomeric
650 facultative heterochromatin in *Neurospora crassa*. *Proceedings of the National*
651 *Academy of Sciences*, 113(52), pp.15048–15053.
652 Kumaran, R., Yang, S.-Y. & Leu, J.-Y., 2013. Characterization of Chromosome Stability in
653 Diploid, Polyploid and Hybrid Yeast Cells. *PLOS ONE*, 8(7), p.e68094.
654 Langmead, B. & Salzberg, S.L., 2012. Fast gapped-read alignment with Bowtie 2. *Nat*
655 *Methods*, 9(4), pp.357–359.
656 Li, H., 2011. A statistical framework for SNP calling, mutation discovery, association mapping
657 and population genetical parameter estimation from sequencing data. *Bioinformatics*,
658 27(21), pp.2987–2993.
659 Linde, C.C., Zhan, J. & McDonald, B.A., 2002. Population Structure of Mycosphaerella
660 graminicola: From Lesions to Continents. *Phytopathology*, 92(9), pp.946–955.
661 Ma, L.-J. et al., 2010. Comparative genomics reveals mobile pathogenicity chromosomes in
662 Fusarium. *Nature*, 464(7287), pp.367–373.
663 McClintock, B., 1938. The Production of Homozygous Deficient Tissues with Mutant
664 Characteristics by Means of the Aberrant Mitotic Behavior of Ring-Shaped
665 Chromosomes. *Genetics*, 23(4), pp.315–376.
666 McClintock, B., 1941. The Stability of Broken Ends of Chromosomes in Zea Mays. *Genetics*,
667 26(2), pp.234–282.
668 McDonald, B. a. & Martinez, J.P., 1991. Chromosome length polymorphisms in a Septoria
669 tritici population. *Current Genetics*, 19(4), pp.265–271.
670 McDonald, M.C. et al., 2016. Utilizing Gene Tree Variation to Identify Candidate Effector
671 Genes in Zymoseptoria tritici. *G3 (Bethesda, Md.)*, 6(4), pp.779–91.
672 McGranahan, N. et al., 2012. Cancer chromosomal instability: therapeutic and diagnostic
673 challenges. *EMBO Rep*, 13(6), pp.528–538.

674 Mehrabi, R., Taga, M. & Kema, G.H.J., 2007. Electrophoretic and cytological karyotyping of
675 the foliar wheat pathogen Mycosphaerella graminicola reveals many chromosomes
676 with a large size range. *Mycologia*, 99(6), pp.868–76.
677 Miao, V., Covert, S. & VanEtten, H., 1991. A fungal gene for antibiotic resistance on a
678 dispensable ("B") chromosome. *Science*, 254(5039), pp.1773–1776.
679 Miao, V.P., Covert, S.F. & VanEtten, H.D., 1991. A fungal gene for antibiotic resistance on a
680 dispensable (" B") chromosome. *Science*, 254(5039), p.1773.
681 Murnane, J.P., 2012. Telomere dysfunction and chromosome instability. *Mutation*
682 *Research/Fundamental and Molecular Mechanisms of Mutagenesis*, 730(1), pp.28–36.
683 Persoons, A. et al., 2014. Patterns of genomic variation in the poplar rust fungus
684 Melampsora larici-populina identify pathogenesis-related factors. *Frontiers in Plant*
685 *Science*, 5(September), p.450.
686 Petit-Houdenot, Y. & Fudal, I., 2017. Complex Interactions between Fungal Avirulence Genes
687 and Their Corresponding Plant Resistance Genes and Consequences for Disease
688 Resistance Management. *Frontiers in Plant Science*, 8(June).
689 Plissonneau, C. & Stürchler, A., 2016. The Evolution of Orphan Regions in Genomes of a
690 Fungal Pathogen of Wheat. , 7(5).
691 Poláková, S. et al., 2009. Formation of new chromosomes as a virulence mechanism in yeast
692 Candida glabrata. *Proceedings of the National Academy of Sciences of the United States*
693 *of America*, 106(8), pp.2688–2693.
694 Ponomarenko, A., Goodwin, S.B. & Kema, G.H.J., 2011. Septoria tritici blotch (STB) of wheat
695 Septoria tritici blotch (STB) of wheat. *Plant Health Instructor*, (Figure 2), pp.1–7.
696 Quinlan, A.R. & Hall, I.M., 2010. BEDTools: a flexible suite of utilities for comparing genomic
697 features. *Bioinformatics*, 26(6), pp.841–842.
698 Rudd, J.J. et al., 2015. Transcriptome and metabolite profiling of the infection cycle of
699 Zymoseptoria tritici on wheat reveals a biphasic interaction with plant immunity
700 involving differential pathogen chromosomal contributions and a variation on the
701 hemibiotrophic lifestyle def. *Plant physiology*, 167(3), pp.1158–85.
702 Schneider, C. a, Rasband, W.S. & Eliceiri, K.W., 2012. NIH Image to ImageJ: 25 years of image
703 analysis. *Nature Methods*, 9(7), pp.671–675.
704 Schotanus, K. et al., 2015. Histone modifications rather than the novel regional centromeres
705 of Zymoseptoria tritici distinguish core and accessory chromosomes. *Epigenetics &*
706 *chromatin*, 8, p.41.
707 Selmecki, A., Forche, A. & Berman, J., 2010. Genomic plasticity of the human fungal
708 pathogen Candida albicans. *Eukaryotic Cell*, 9(7), pp.991–1008.
709 Slee, R.B. et al., 2012. Cancer-associated alteration of pericentromeric heterochromatin may
710 contribute to chromosome instability. *Oncogene*, 31(27), pp.3244–53.
711 Southern, E.M., 1975. Detection of specific sequences among DNA fragments separated by
712 gel electrophoresis. *Journal of Molecular Biology*, 98(3), pp.503–517.
713 Sprouffske, K. & Wagner, A., 2016. Growthcurver: an R package for obtaining interpretable
714 metrics from microbial growth curves. *BMC Bioinformatics*, 17(1), p.172.
715 Stewart, E.L. et al., 2016. An improved method for measuring quantitative resistance to the
716 wheat pathogen Zymoseptoria tritici using high throughput automated image analysis.
717 *Phytopathology*.
718 Stukenbrock, E.H. et al., 2011. The making of a new pathogen: insights from comparative
719 population genomics of the domesticated wheat pathogen Mycosphaerella graminicola
720 and its wild sister species. *Genome research*, 21(12), pp.2157–66.
721 Stukenbrock, E.H. et al., 2010. Whole-genome and chromosome evolution associated with

722 host adaptation and speciation of the wheat pathogen Mycosphaerella graminicola.
723 *PLoS genetics*, 6(12), p.e1001189.
724 Stukenbrock, E.H. & Dutheil, J.Y., 2018. Fine-scale recombination maps of fungal plant
725 pathogens reveal dynamic recombination landscapes and intragenic hotspots. *Genetics*,
726 208(3), pp.1209–1229.
727 Thorvaldsdóttir, H., Robinson, J.T. & Mesirov, J.P., 2013. Integrative Genomics Viewer (IGV):
728 High-performance genomics data visualization and exploration. *Briefings in*
729 *Bioinformatics*, 14(2), pp.178–192.
730 Torriani, S.F.F. et al., 2015. Zymoseptoria tritici: A major threat to wheat production,
731 integrated approaches to control. *Fungal Genetics and Biology*, 79, pp.8–12.
732 Tsuge, T. et al., 2016. Evolution of pathogenicity controlled by small, dispensable
733 chromosomes in Alternaria alternata pathogens. *Physiological and Molecular Plant*
734 *Pathology*, 95, pp.27–31.
735 Vlaardingerbroek, I. et al., 2016. Dispensable chromosomes in Fusarium oxysporum f . sp
736 lycopersici . *Molecular Plant Pathology*, pp.1–12.
737 Wang, B. et al., 2006. Genetic variation and population structure of Fusarium oxysporum
738 f.sp. vasinfectum in Australia. *Plant Pathology*, 55(6), pp.746–755.
739 Wittenberg, A.H.J. et al., 2009. Meiosis drives extraordinary genome plasticity in the haploid
740 fungal plant pathogen Mycosphaerella graminicola. *PloS one*, 4(6), p.e5863.
741 Zhan, J. & McDonald, B.A., 2011. Thermal adaptation in the fungal pathogen Mycosphaerella
742 graminicola. *Molecular Ecology*, 20(8), pp.1689–1701.
743 Zhan, J., Pettway, R.E. & McDonald, B.A., 2003. The global genetic structure of the wheat
744 pathogen Mycosphaerella graminicola is characterized by high nuclear diversity, low
745 mitochondrial diversity, regular recombination, and gene flow. *Fungal Genetics and*
746 *Biology*, 38(3), pp.286–297.
747 Zhong, Z. et al., 2017. A small secreted protein in Zymoseptoria tritici is responsible for
748 avirulence on wheat cultivars carrying the Stb6 resistance gene. *New Phytologist*,
749 214(2), pp.619–631.
750 Zhu, Y.O. et al., 2014. Precise estimates of mutation rate and spectrum in yeast. *Proceedings*
751 *of the National Academy of Sciences* , 111(22), pp.E2310–E2318.
752

753 **Supplement**

754

755 **Table S1: List of primers used for screening for accessory chromosomes in *Z. tritici* and *Z.***
756 ***ardabiliae*.**

Primer name	Sequence (5' to 3')	Coordinates	Expected PCR product length (bp)
Telomere L			
oES2084_Tel**14**L_F	TCGACCGAGGGTCAGAGATT	52785.. 52804	150
oES2085_Tel**14**L_R	GTGCGAACCGACATCCACTA	52934.. 52915	
oES2088_Tel**15**L_F	AGACGAAGGCACCACCAGAT	29301.. 29320	253
oES2089_Tel**15**L_R	GTGCATCCTCATCCCCCTTA	29553.. 29534	
oES2092_Tel**16**L_F	TCGGAAACACCGGTCTAAGC	25143.. 25162	344
oES2093_Tel**16**L_R	ATAGAGGCGGTCGACGAGAA	25486.. 25467	
oES2096_Tel**17**L_F	GGCTTCTGCCATCAGAGCTT	88346.. 88365	451
oES2097_Tel**17**L_R	CAACTTCCTCCGCTTTGCTC	88796.. 88777	
oES2100_Tel**18**L_F	GTTTTCTCCCTGCACCTTGC	14259.. 14278	540
oES2101_Tel**18**L_R	TATGGCACCTCCGAACAATG	14798.. 14779	
oES2104_Tel**19**L_F	CAAGACGGCTCCCTTTCATC	19008.. 19027	652
oES2105_Tel**19**L_R	AGGAGGAACCATCGAAGCAG	19659.. 19640	
oES2108_Tel**20**L_F	CGGTTCAGATCAGGTGCAAA	6803.. 6822	743
oES2109_Tel**20**L_R	CGTGGAAGAGCATCGACAAG	7545.. 7526	
oES2112_Tel**21**L_F	GTCCAGCCATCGATTTTCGT	46192.. 46211	849
oES2113_Tel**21**L_R	GTCGGGATATGTGCGAGTGA	47040.. 47021	
Telomere R			
oES2086_Tel**14**R_F	CTCCGCTTTGCTTTCCGTAG	722989..723008	896
oES2087_Tel**14**R_R	GTCCGCAAGTGACAAATCCA	723884..723865	
oES2090_Tel**15**R_F	CTACCGCTCGGTTCCAAAAG	581237..581256	799
oES2091_Tel**15**R_R	TTGGGAAACTGTCCTGACCA	582035..582016	
oES2094_Tel**16**R_F	CCAGATTTGGGAATGGGTGT	587178..587197	704
oES2095_Tel**16**R_R	GCTGACGAACTGCTCGAAGA	587881..587862	
oES2098_Tel**17**R_F	AGGTGGTGGATTCGGGATTA	554580..554599	601
oES2099_Tel**17**R_R	CTGCATGCTCTCGATTACGC	555180..555161	
oES2102_Tel**18**R_F	GAGAATGTGGTCGCGGAGAT	521319..521338	500
oES2103_Tel**18**R_R	GAGCCCTTCACCAACACACA	521818..521799	
oES2106_Tel**19**R_F	ACATCCTCCACTCGGCTTGT	531276..531295	398
oES2107_Tel**19**R_R	AGCTACGACGCCATCACCTT	531673..531654	
oES2110_Tel**20**R_F	GGCACCAACTGCACATGATT	437575..437594	292
oES2111_Tel**20**R_R	ACATGCGAGCTGGATCTGAA	437866..437847	
oES2114_Tel**21**R_F	TTGCAGCTCTTGGAGCGATA	379214..379233	202
oES2115_Tel**21**R_R	CCCAGTCGTAATGGGAAGGA	379415..379396	
Centromere			
oES1986_Chr**21**_F	CCTCGCCACCATGTTATACC	306266..306285	294

oES1987_Chr**21**_R	CGCACCTACAGTCCGAAATC	306559..306540	
oES1988_Chr**20**_F	ATGCGAATTGGAGCAGCTAC	118378..118397	500
oES1989_Chr**20**_R	ATCGACGGTGTGCATCTTAC	118877..118858	
oES2002_Chr**19**_F	ACATGGCATCCTGGATTGTC	200830..200849	697
oES2003_Chr**19**_R	ACGAGCTTCTGTTTCCACTG	201526..201507	
oES1992_Chr**18**_F	CCTTCATGCCGGTGCTTTAC	188047..188066	908
oES1993_Chr**18**_R	GATGCCATCGGTCCATAGTG	188954..188935	
oES1994_Chr**17**_F	CACGAGCGACAAGGACTATC	385216..385235	1204
oES1995_Chr**17**_R	AGTGCCCGAGTTTCAACATC	386419..386400	
oES1996_Chr**16**_F	TGCACTAACGCCTCAACTAC	300338..300357	1501
oES1997_Chr**16**_R	TGGCTCTTTGCACTCAAGAC	301838..301819	
oES1998_Chr**15**_F	TTCGAATGCCGGTCATACAC	357359..357378	1991
oES1999_Chr**15**_R	GCAAACCACGAAGCTTTCTC	359349..359330	
oES2000_Chr**14**_F	AAGTGGAAGCGCCCATAATC	106407..106426	2520
oES2001_Chr**14**_R	GACCTCACTTCGCCACATAG	108926..108907	
Za17			
oES2399_unitig**24**_F	TCGGACTAGGAGACCGAATG	233390..233409	94
oES2400_unitig**24**_R	TTTGCGAAGACGCCAGAAAC	233483..233464	
oES2401_unitig**27**_F	CGTAGCGGTAGGAGTATTCG	265475..265494	159
oES2402_unitig**27**_R	CGGCTACTTACTAGGCCTTC	265633..265614	
oES2403_unitig**49**_F	GATGCTGACCGGTATCATGG	300139..300158	269
oES2404_unitig**49**_R	CAGCAACAGGTGCATTAGTG	300407..300388	
oES2405_unitig**51**_F	AACTTCGTCCACAGTCCTAC	71090..71109	350
oES2406_unitig**51**_R	GAAGCTACATCGGGTGATTC	71439..71420	
oES2407_unitig**99**_F	TGTGAACCCGCAATGATCCC	137946..137965	420
oES2408_unitig**99**_R	GGCGTTGAGCAGACCTGTAG	138365..138346	
oES2409_unitig**112**_F	ACCTCGCGTGAAGATGTAAG	89655..89674	491
oES2410_unitig**112**_R	CTGCGCCAGAGTTGAAAGTC	90145..90126	
Probes for Southern analyses			
oES3018_Chr**17**_F	GACGGGATCTATGCTACAGG	210784..210803	1515
oES3019_Chr**17**_R	ACCGCACCGTTGGCTATTTG	212298..212279	
oES3020_Chr**21**_F	GCTTCTTCCCAGCATCTGAC	276789..276808	1597
oES3021_Chr**21**_R	CGGAAGCACAGGCAATATCG	278385..278366	
oES3022_Chr**12**_F	TAGACCCGGTCTGGAGAATC	804683..804702	1519
oES3023_Chr**12**_R	TCGACTTCGGGTGACTTGAG	806201..806182	

757

758 **Table S2: List of chromosome-loss strains identified in the *in vitro* and *in planta***
759 **experiments.** Strains described in detail in the main text are highlighted in **bold**.

Experiment	Strain name	Chromosome(s) lost	Strain name in main text	Method used to confirm chromosome loss
progenitor	**Zt09**	**18**	**Zt09**[3)]	**PCR, PFGE**[1)]**, WGS**[2)]
progenitor	**IPO323**	**-**	**IPO323**[4)]	**PCR, PFGE, WGS**
progenitor	**STIR04 1.1.1**	**-**	**Za17**	**PCR, PFGE, WGS**
Zt09 *in vitro* liquid culture 18°C				
	Zt09_18_1.1.38	**14 (18)**	**Zt09Δ14**[3)]	**PCR, PFGE, WGS**
	Zt09_18_1.1.45	**15 (18)**	**Zt09Δ15**	**PCR, PFGE, WGS**
	Zt09_18_1.1.51	14 (18)		
	Zt09_18_1.1.71	**21 (18)**	**Zt09Δ21**[3)]	**PCR, PFGE, WGS**
	Zt09_18_1.1.85	16 (18)		PCR, PFGE
	Zt09_18_1.1.95	14 (18)		PCR, PFGE
	Zt09_18_2.1.3	16 (18)		PCR, PFGE
	Zt09_18_2.1.4	14 (18)		PCR, PFGE
	Zt09_18_2.1.21	15 (18)		PCR, PFGE
	Zt09_18_2.1.24	15 (18)		PCR, PFGE
	Zt09_18_2.1.33	14 (18)		PCR, PFGE
	Zt09_18_2.1.64	14 (18)		PCR, PFGE
	Zt09_18_2.1.68	16 (18)		PCR, PFGE
	Zt09_18_2.1.73	20 (18)		PCR, PFGE
	Zt09_18_2.1.79	16 (18)		PCR, PFGE
	Zt09_18_2.1.85	14 (18)		PCR, PFGE
	Zt09_18_1.2.4	15 (18)		PCR, PFGE
	Zt09_18_1.2.18	**20 (18)**	**Zt09Δ20**	**PCR, PFGE, WGS**
	Zt09_18_1.2.40	15 (18)		PCR
	Zt09_18_1.2.48	15 (18)		PCR
	Zt09_18_1.2.86	15 (18)		PCR
	Zt09_18_1.2.89	16 (18)		PCR
	Zt09_18_1.2.93	14 (18)		PCR
	Zt09_18_2.2.6	14 (18)		PCR
	Zt09_18_2.2.38	14 (18)		PCR
	Zt09_18_2.2.43	15 (18)		PCR
	Zt09_18_2.2.64	14 (18)		PCR
	Zt09_18_2.2.70	16 (18)		PCR
	Zt09_18_2.2.74	16 (18)		PCR
	Zt09_18_1.3.40	14 (18)		PCR
	Zt09_18_1.3.41	14 (18)		PCR
	Zt09_18_1.3.92	16 (18)		PCR
	Zt09_18_2.3.21	14 (18)		PCR
	Zt09_18_2.3.41	14 (18)		PCR
	Zt09_18_2.3.49	14 (18)		PCR
	Zt09_18_2.3.53	14 (18)		PCR
	Zt09_18_2.3.85	14 (18)		PCR
	Zt09_18_2.3.86	16 (18)		PCR

Zt09 *in vitro* liquid culture 28°C				
	Zt09_28_1.1.1	14 (18)		PCR
	Zt09_28_1.1.2	14 (18)		PCR
	Zt09_28_1.1.4	14 (18)		PCR
	Zt09_28_1.1.5	14 (18)		PCR
	Zt09_28_1.1.6	14 (18)		PCR
	Zt09_28_1.1.8	14 (18)		PCR
	Zt09_28_1.1.10	14 (18)		PCR
	Zt09_28_1.1.11	14,21 (18)		PCR, PFGE
	Zt09_28_1.1.12	14,20 (18)		PCR, PFGE
	Zt09_28_1.1.13	14 (18)		PCR
	Zt09_28_1.1.14	14 (18)		PCR
	Zt09_28_1.1.15	14 (18)		PCR
	Zt09_28_1.1.17	14 (18)		PCR
	Zt09_28_1.1.19	14,20,21 (18)	**Zt09 28-1**	**PCR, PFGE, WGS**
	Zt09_28_1.1.21	14 (18)		PCR
	Zt09_28_2.1.2	19 (18)		PCR
	Zt09_28_2.1.3	14 (18)		PCR
	Zt09_28_2.1.4	14 (18)		PCR
	Zt09_28_2.1.6	14 (18)		PCR
	Zt09_28_2.1.7	14 (18)		PCR
	Zt09_28_2.1.8	14 (18)		PCR
	Zt09_28_2.1.9	14 (18)		PCR
	Zt09_28_2.1.10	14 (18)		PCR
	Zt09_28_2.1.11	14 (18)		PCR
	Zt09_28_2.1.12	14 (18)		PCR
	Zt09_28_2.1.14	14,20 (18)		PCR
	Zt09_28_2.1.15	14 (18)		PCR
	Zt09_28_2.1.16	14 (18)		PCR
	Zt09_28_2.1.17	14 (18)		PCR
	Zt09_28_2.1.18	14 (18)		PCR
	Zt09_28_2.1.19	14 (18)		PCR
	Zt09_28_2.1.21	14,20,21 (18)		PCR
	Zt09_28_2.1.22	20 (18)		PCR
	Zt09_28_2.1.24	14,16 (18)		PCR
	Zt09_28_2.1.25	14 (18)		PCR
	Zt09_28_2.1.26	14,20 (18)		PCR
	Zt09_28_2.1.27	14 (18)		PCR
	Zt09_28_2.1.28	14 (18)		PCR
	Zt09_28_2.1.29	14 (18)		PCR
	Zt09_28_2.1.31	14 (18)		PCR
	Zt09_28_2.1.33	14 (18)		PCR
	Zt09_28_2.1.34	14 (18)		PCR
	Zt09_28_2.1.35	14 (18)		PCR
	Zt09_28_2.1.37	14 (18)		PCR
	Zt09_28_2.1.38	14,20 (18)		PCR, PFGE
	Zt09_28_2.1.39	21 (18)		PCR, PFGE
	Zt09_28_2.1.40	14 (18)		PCR
	Zt09_28_2.1.41	14 (18)		PCR

	Zt09_28_2.1.42	14 (18)		PCR
	Zt09_28_1.2.1	14,20 (18)		PCR
	Zt09_28_1.2.2	14 (18)		PCR
	Zt09_28_1.2.3	14 (18)		PCR
	Zt09_28_1.2.4	14,15,16,19,20 (18)	**Zt09 28-2**	**PCR, PFGE, WGS**
	Zt09_28_1.2.5	14 (18)		PCR
	Zt09_28_1.2.6	14 (18)		PCR
	Zt09_28_1.2.7	14,16 (18)	**Zt09 28-3**	**PCR, PFGE, WGS**
	Zt09_28_1.2.8	14 (18)		PCR
	Zt09_28_1.2.9	14 (18)		PCR
	Zt09_28_1.2.10	14 (18)		PCR
	Zt09_28_1.2.11	14 (18)		PCR
	Zt09_28_1.2.12	14,15 (18)		PCR, PFGE
	Zt09_28_1.2.15	14 (18)		PCR
	Zt09_28_1.2.16	14 (18)		PCR
	Zt09_28_1.2.17	14 (18)		PCR
	Zt09_28_1.2.18	14,15,20,21 (18)	**Zt09 28-4**	**PCR, PFGE, WGS**
	Zt09_28_1.2.19	14,16 (18)		PCR, PFGE
	Zt09_28_1.2.20	14,21 (18)		PCR, PFGE
	Zt09_28_1.2.21	14 (18)		PCR
	Zt09_28_1.2.22	14 (18)		PCR
	Zt09_28_1.2.23	14,20 (18)		PCR, PFGE
	Zt09_28_1.2.24	14 (18)		PCR
	Zt09_28_1.2.25	14 (18)		PCR
	Zt09_28_1.2.26	14 (18)		PCR
	Zt09_28_1.2.27	14,15 (18)		PCR, PFGE
	Zt09_28_1.2.28	14 (18)		PCR
	Zt09_28_1.2.29	14 (18)		PCR
	Zt09_28_1.2.30	14 (18)		PCR
	Zt09_28_1.2.31	14 (18)		PCR
	Zt09_28_1.2.32	14 (18)		PCR
	Zt09_28_2.2.1	14 (18)		PCR
	Zt09_28_2.2.2	14 (18)		PCR
	Zt09_28_2.2.3	15 (18)		PCR
	Zt09_28_2.2.4	14 (18)		PCR
	Zt09_28_2.2.5	14 (18)		PCR
	Zt09_28_2.2.6	15 (18)		PCR
	Zt09_28_2.2.7	14 (18)		PCR
	Zt09_28_2.2.10	14 (18)		PCR
	Zt09_28_2.2.11	14 (18)		PCR
	Zt09_28_2.2.12	14,16 (18)		PCR
	Zt09_28_2.2.13	14 (18)		PCR
	Zt09_28_2.2.14	14,16 (18)		PCR
	Zt09_28_2.2.15	14,20 (18)		PCR
	Zt09_28_2.2.16	14,15 (18)	**Zt09 28-5**	**PCR, PFGE, WGS**
	Zt09_28_2.2.17	14 (18)		PCR
	Zt09_28_2.2.18	14,16 (18)		PCR
	Zt09_28_2.2.19	14 (18)		PCR
	Zt09_28_2.2.20	14 (18)		PCR
	Zt09_28_2.2.21	14 (18)		PCR
	Zt09_28_2.2.22	14,15 (18)		PCR

	Zt09_28_2.2.23	14 (18)		PCR
	Zt09_28_2.2.24	14 (18)		PCR
	Zt09_28_2.2.25	14 (18)		PCR
	Zt09_28_2.2.26	14,20 (18)		PCR
	Zt09_28_2.2.27	19 (18)		PCR
	Zt09_28_2.2.28	14 (18)		PCR
	Zt09_28_1.3.1	14 (18)		PCR
	Zt09_28_1.3.2	14 (18)		PCR
	Zt09_28_1.3.4	14,20 (18)		PCR, PFGE
	Zt09_28_1.3.5	16,20 (18)		PCR, PFGE
	Zt09_28_1.3.6	14 (18)		PCR
	Zt09_28_1.3.7	14,16 (18)		PCR, PFGE
	Zt09_28_1.3.8	14,20 (18)		PCR
	Zt09_28_1.3.11	14 (18)		PCR
	Zt09_28_1.3.13	14 (18)		PCR
	Zt09_28_1.3.14	14,20,21 (18)		PCR
	Zt09_28_1.3.15	14 (18)		PCR
	Zt09_28_1.3.17	14 (18)		PCR
	Zt09_28_1.3.18	14 (18)		PCR
	Zt09_28_1.3.19	14 (18)		PCR
	Zt09_28_1.3.20	14 (18)		PCR
	Zt09_28_1.3.22	14 (18)		PCR
	Zt09_28_1.3.24	14,15 (18)		PCR
	Zt09_28_1.3.27	14 (18)		PCR
	Zt09_28_1.3.28	14 (18)		PCR
	Zt09_28_2.3.1	14,20 (18)		PCR
	Zt09_28_1.3.3	14 (18)		PCR
	Zt09_28_1.3.5	14 (18)		PCR
	Zt09_28_1.3.6	14 (18)		PCR
	Zt09_28_1.3.7	14 (18)		PCR
	Zt09_28_1.3.9	14 (18)		PCR
	Zt09_28_1.3.11	14 (18)		PCR
	Zt09_28_1.3.12	14 (18)		PCR
	Zt09_28_1.3.13	14 (18)		PCR
	Zt09_28_1.3.14	14,21 (18)		PCR
	Zt09_28_1.3.15	14 (18)		PCR
	Zt09_28_1.3.17	14 (18)		PCR
	Zt09_28_1.3.19	14 (18)		PCR
	Zt09_28_1.3.20	14 (18)		PCR
	Zt09_28_1.3.22	14 (18)		PCR
	Zt09_28_1.3.26	14 (18)		PCR
	Zt09_28_1.3.27	14,15 (18)		PCR
	Zt09_28_1.3.28	14 (18)		PCR
	Zt09_28_1.3.29	14 (18)		PCR
	Zt09_28_1.3.30	14 (18)		PCR
	Zt09_28_1.3.32	14 (18)		PCR
	Zt09_28_1.3.33	14,19 (18)		PCR
	Zt09_28_1.3.35	14 (18)		PCR
	Zt09_28_1.3.36	14 (18)		PCR

Zt09 *in vitro* on plate 18°C				
	2-08-005	16 (18)		PCR
	2-09-005	16 (18)		PCR
	2-14-005	16 (18)		PCR
	2-17-005	16 (18)		PCR
	2-01-005	21 (18)		PCR
IPO323 *in planta*				
	A#101	**14**	**IPO323Δ14**[4)]	**PCR, PFGE, WGS**
	A#52	15		PCR
	B#56	**15**	**IPO323Δ15**[4)]	**PCR, PFGE, WGS**
	B#181	15		PCR
	PycB F15 13	15		PCR
	PycB F15 52	15		PCR
	PycB F30 6	15		PCR
	PycB E 29 57	**16**	**IPO323Δ16**[4)]	**PCR**
	PycA E10#17	18		PCR
	B#152	**18**	**IPO323Δ18**[4)]	**PCR, PFGE, WGS**
	PycB F15 1	18		PCR
	PycB F15 75	18		PCR
	PycB F15 83	18		PCR
	PycB F30 43	18		PCR
	PycB F30 90	18		PCR
	B#59	**19**	**IPO323Δ19**[4)]	**PCR, PFGE, WGS**
	PycB F15 79	19		PCR
Za17 in vitro liquid culture 18°C				
	Za17_2.46	**unitig 24**	**ZaΔ24**	**PCR, PFGE, WGS**
	Za17_2.61	**unitig 49**	**ZaΔ49**	**PCR, PFGE, WGS**
	Za17_2.69	**unitig 51**	**ZaΔ51**	**PCR, PFGE, WGS**
	Za17_2.81	unitig 49		PCR, PFGE
	Za17_3.38	unitig 51		PCR, PFGE

760

761 [1)] Pulsed-field gel electrophoresis

762 [2)] Whole genome sequencing

763 [3)]Strains used for *in vitro* growth assay

764 [4)]Strains used for *in vitro* and *in planta* phenotyping

765 **Table S3: Chromosome variation of sequenced Zt09-derived strains grown at 28°C.** Absent
766 sequences at the ends of each chromosome (left (L) or right (R) arm) are indicated, as well as
767 the complete absence or a duplication of a chromosome.

Chromosome	Zt09 28-1	Zt09 28-2	Zt09 28-3	Zt09 28-4	Zt09 28-5
1			[2)] internal tel 183,500		
2			L (5 kb) new tel 2 breakpoints R (4 kb) new tel		
3		R (10 kb) attached to chr 13			
4					L (10 kb) new tel
5	R (35 kb)[1)] new tel	R (35 kb)[1)] new tel	R (35 kb)[1)] new tel	R (35 kb)[1)] new tel	R (35 kb)[1)] new tel
6			R (2 kb) new tel		
7					
8	R (200 bp)				
9	R (16 kb) new tel	R (3 kb) new tel			
10			L (27 kb) new tel		L (7 kb)
11			R (2.5 kb) new tel		
12					
13		R attached to chr 3		R (1.5 kb) new tel	
14	absent	absent	absent	absent	absent
15	R (350 bp) new tel	absent		absent	absent
16		absent	absent		
17		**duplicated**	L (60 kb) new tel R (1kb)	**duplicated** [2)] internal tel 54,000	
18	absent	absent	absent	absent	absent
19		absent	L (22 kb) new tel		
20	absent	absent		absent	**duplicated**
21	absent	L (400 bp) [2)] internal tel 32,000		absent	

768

769 [1)] The 35 kb sequence missing on the right arm of chromosome five is already absent in the
770 progenitor strain Zt09. Discordant reads suggest a new telomere formation indicated as
771 'new tel'.
772 [2)] Coordinates of cases where new telomeres were not located at chromosome breakpoints.

773 **Table S4: Location and annotation of SNPs and INDELs found in the sequenced**
774 **chromosome-loss strains.** Listed are SNPs that deviate in the chromosome loss strains from
775 the respective corresponding ancestral strain Zt09, IPO323 or Za17. Also listed are the SNPs
776 that differ between the ancestral strains Zt09 and IPO323 and the reference genome.
777 Polymorphisms in coding regions are indicated in **bold**.

Strain	Species	SNP (total)	SNP (coding)	Coordinates	Mutation	Gene annotation
Zt09Δ14	*Z. tritici*	0	0			
Zt09Δ15	*Z. tritici*	0	0			
Zt09Δ20	*Z. tritici*	2	0	chr 10: 1,547,664 chr 15: 639,408	A -> G TTA ->TTATA	
Zt09Δ21	*Z. tritici*	0	0			
IPO323Δ14	*Z. tritici*	1	**1**	**chr 1: 4,492,118**	**G -> C (non-syn)**	**hypoth. protein**
IPO323Δ15	*Z. tritici*	2	0	chr 6: 746,848 chr 10: 517,128	G -> C 17 bp del	
IPO323Δ18	*Z. tritici*	3	**2**	**chr 3: 3,145,507** **chr 10: 735,717** chr 19: 395,097	**C -> T (non-syn)** **9 bp del (in frame)** G -> A	**zinc-finger** **histidine-kinase**
IPO323Δ19	*Z. tritici*	1	0	chr 9: 1,937,298	A -> G	
Za17Δ24	*Z. ardabiliae*	0	0			
Za17Δ49	*Z. ardabiliae*	0	0			
Za17Δ51	*Z. ardabiliae*	0	0			
Zt09	*Z. tritici*	17	5	chr 1: 125 **chr 1: 4,373,965** chr 2: 1,137,727 chr 3: 831,118 chr 3: 2,780,000 **chr 4: 807,372** chr 5: 690, 228 **chr 5: 1,102,332** chr 5: 1,814,335 chr 5: 1,814, 365 chr 7: 2,644,548 chr 9: 2,142,382 chr 10: 1,630,016 **chr 11: 223,110** chr 12: 415,459 chr 12: 935,185 **chr 12: 979,588**	C -> A **CA -> AC (non-syn)** G -> A A -> G A -> T **AG -> AAGGG** T -> C **C -> T (syn)** GT -> GTT T -> C A -> G T -> A G -> T **404 bp deletion (in frame)** C -> T TG -> T **A -> G (syn)**	**hypoth. protein** **pred. protein** **hypoth. protein** **white collar-1[1)]** **hypoth. protein**
IPO323	*Z. tritici*	22	3	**chr 1: 4,373,965** chr 2: 400,119 chr 2: 1,137,727 chr 2: 1,459,200 chr 3: 831,118 **chr 3: 2,633,702** chr 4: 999,781 chr 5: 690, 228 chr 5: 1,814,335 chr 5: 1,814, 365	**CA -> AC (non-syn)** C -> T G -> A T -> C A -> G **AGGCGG -> AGG (in frame)** G -> C T -> C GT -> GTT T -> C	**hypoth. protein** **RNAi gene Qde2**

				chr 7: 2,644,548	A -> G	
				chr 9: 2,142,382	T -> A	
				chr 10: 1,321,821	A -> C	
				chr 10: 1,630,016	G -> T	
				chr 11: 1,063,938	A -> C	
				chr 12: 415,459	C -> T	
				chr 12: 596,261	**G -> A (syn)**	**hypoth. protein**
				chr 12: 605,733	GCTCC -> GC	
				chr 15: 586,233	G -> C	
				chr 16: 245,451	A -> C	
				chr 19: 263,608	A -> C	
				chr 20: 449,279	A -> T	

[1)] Notably, one difference between Zt09 and the reference was a 404 bp deletion (resulting in a truncated, in frame transcript) in the gene of a known regulator of the circadian clock, white collar-1 (Crosthwaite et al. 1997). Zt09 shows phenotypic differences compared to IPO323 and further studies will be conducted to elucidate a possible effect of this deletion in these two strains.

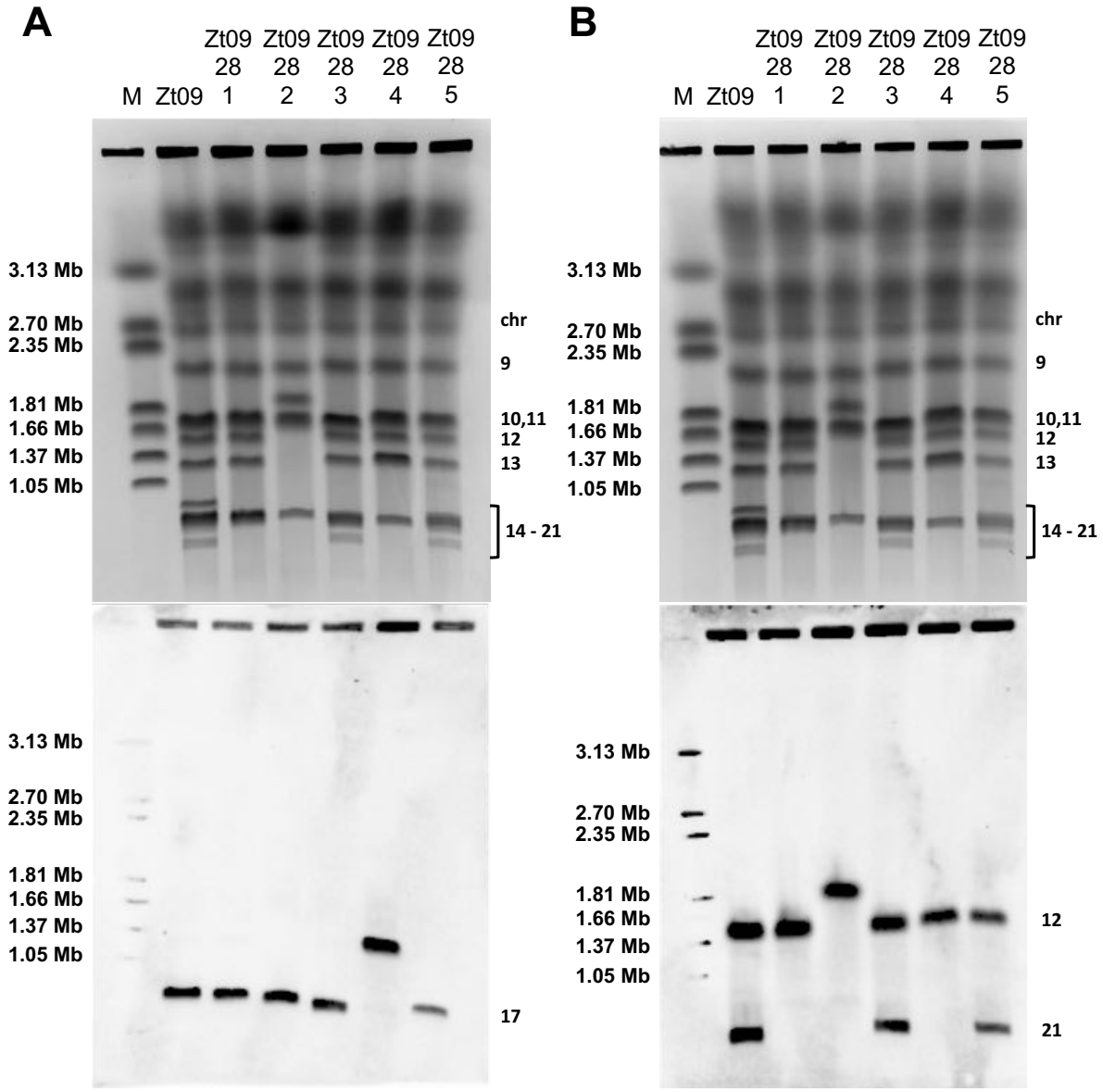

Figure S1: Southern blotting of pulsed-field gels using chromosome-specific probes confirms chromosome fusions. To prove and visualize chromosome fusions in the strains derived from the temperature stress experiment, we conducted PFGE followed by Southern blots with probes specific to the chromosomes, which based on genome data and karyotype analyses, were found to have fused. Panel (A) shows a color-inverted image of the pulsed-field gel (top) and Southern blot (bottom) using a probe specific for chromosome 17. The genomes of all tested strains have chromosome 17, and the genomes of strains Zt09 28-2 and Zt09 28-4 contain a duplicated chromosome 17 (Figure 2C). While in Zt09 28-2 the duplication resulted in two separate copies of the chromosome, the two chromosomes 17 in Zt09 28-4 fused and formed a new ~ 1.2 Mb chromosome. (B) For the second Southern blot, we used probes for chromosomes 12 and 21. Chromosome 21 is absent in the strains Zt09 28-1 and Zt09 28-3 (PFGE, top and Southern analyses, bottom). Genome sequencing shows that chromosome 21 is present in Zt09 28-2 (Figure 2C), however the respective band on the

799 pulsed-field gel is missing. Similarly, chromosomes 12 and 13 are not present in this strain
800 (PFGE, top), while the chromosome sequences are present in the whole genome sequence
801 data. Apparent loss of chromosome 13 can be explained by the fusion of chromosomes 3
802 and 13, as indicated by the sequence analysis (Figure 3). The probes for chromosomes 12
803 and 21 both hybridize to one band in the size of ~1.8 Mb (Southern, bottom) matching the
804 size expected if a chromosome fusion occurred and explaining the absence of their
805 respective 'original' chromosomal bands.

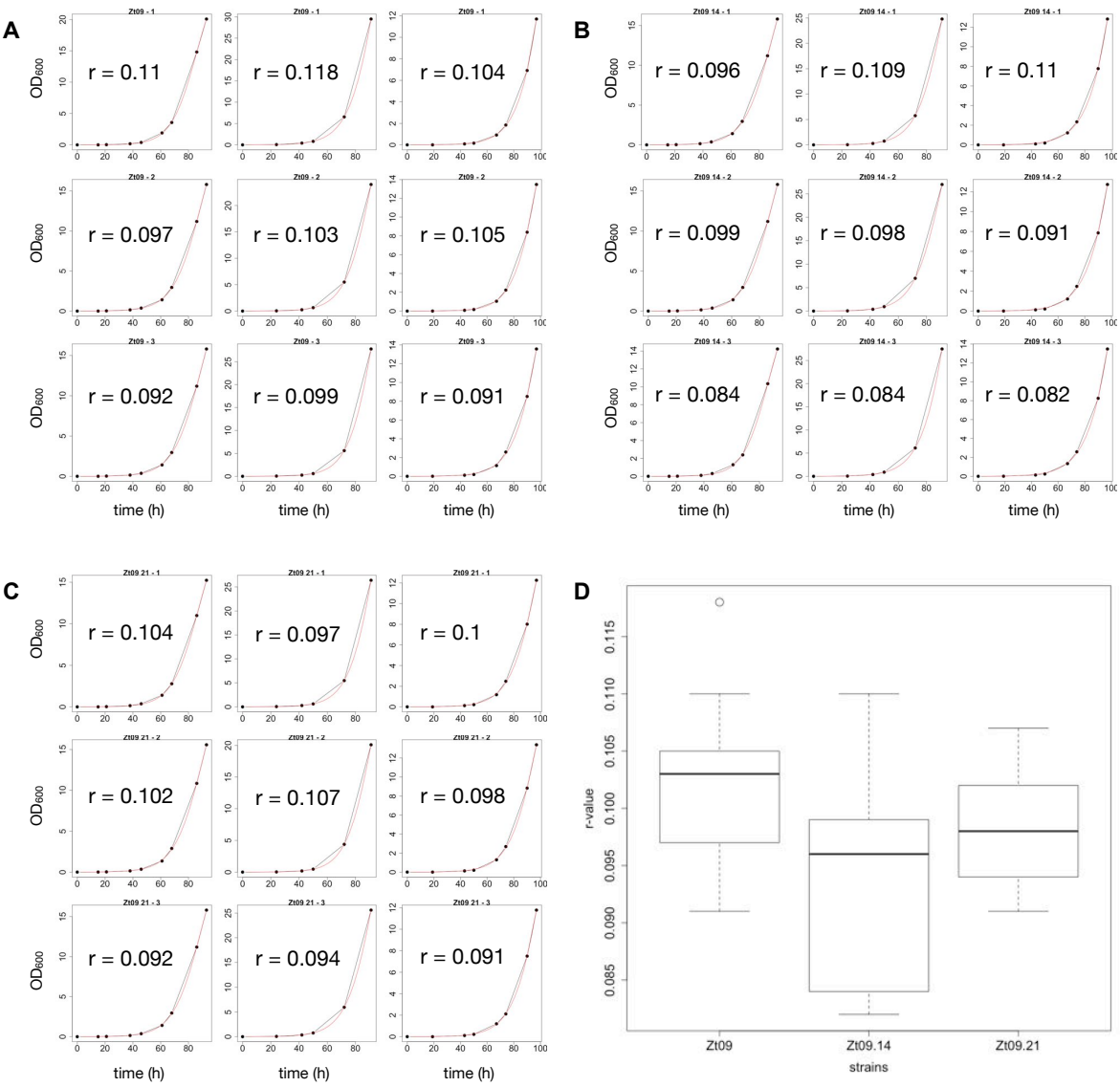

Figure S2: Growth assay of Zt09 and chromosome-loss strains Zt09Δ14 and Zt09Δ21. Three independent growth assays were conducted with the progenitor strain Zt09 (A) and two chromosome-loss strains Zt09Δ14 (B) and Zt09Δ21 (C), representing the loss of the largest and smallest accessory chromosome. Plotted are the fitted growth curves of all replicates and experiments generated with the R package growthcurver. The growth curves are based on OD_{600} measurements. Panel (D) displays a boxplot of all r values of the different strains. There are no significant differences between the growth curves of the three tested strains (Wilcoxon rank-sum test Zt09 – Zt09Δ14: p-value = 0.1443, Zt09 - Zt09Δ21: p-value = 0.3762).

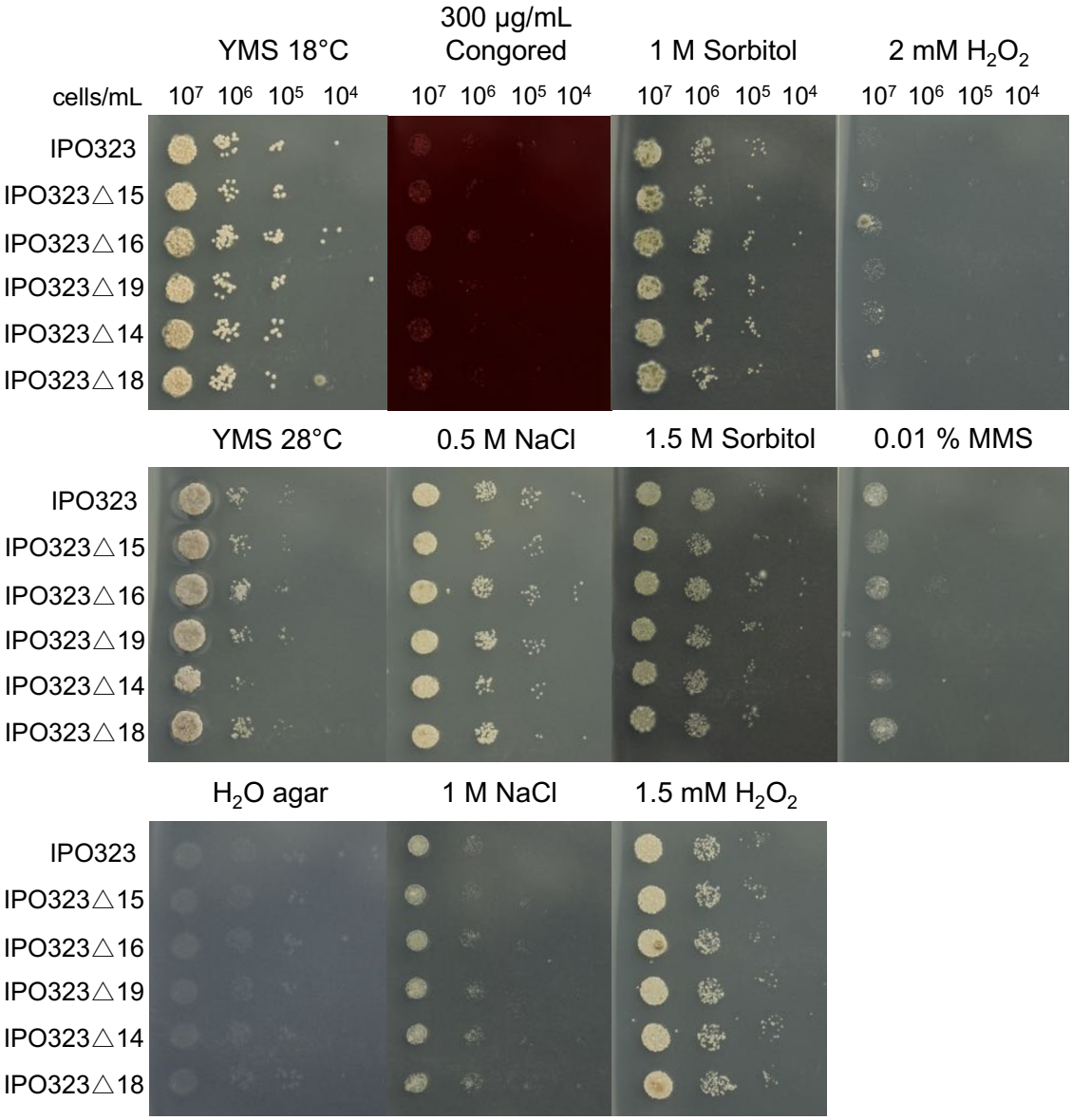

816
817 **Figure S3: *In vitro* stress assays of the *Z. tritici* reference isolate IPO323 and the *in planta***
818 **chromosome-loss strains.** Several *in vitro* stress conditions were tested to assess the effect
819 of accessory chromosome losses on fitness. Five *in planta* chromosome-loss strains were
820 tested, IPO323 was used as the reference strain. We observed no noteworthy differences in
821 growth rate or colony morphology between reference and chromosome-loss strains.

822 **Supplementary text:** Programs and commands used for quality filtering, mapping,
823 visualization, and SNP calling for genome sequencing data and assembly of long-read SMRT
824 sequencing reads of the *Zymoseptoria ardabiliae* reference strain Za17.
825

826 **Quality filtering**
827
828 **Trimmomatic version 0.36** (Bolger et al. 2014)
829
830 java -jar trimmomatic-0.36.jar PE -threads 8 -phred33 R1_sample_1.fastq.gz
831 R2_sample_1.fastq.gz R1_paired.fastq R1_unpaired.fastq R2_paired.fastq R2_unpaired.fastq
832 HEADCROP:10 CROP:149 LEADING:3 TRAILING:3 SLIDINGWINDOW:4:15 MINLEN:50
833
834
835 **Mapping**
836
837 **bowtie2 version 2.1.0** (Langmead & Salzberg 2012)
838
839 bowtie2 -p8 -q -x reference -1 R1_paired.fastq -2 R2_paired.fastq -S sample_1.sam
840
841
842 **Sorting and indexing**
843
844 **samtools version 1.3.1** (Li 2011)
845
846 samtools view -Sb sample_1.sam > sample_1.bam
847
848 samtools sort sample_1.bam > sample_1_sorted.bam
849
850 samtools index sample_1_sorted.bam
851
852
853 **Extraction of discordant reads mapping to different chromosomes**
854
855 samtools view -F 14 -h input_sorted.bam | awk '($3!=$7 && $7!="=")' >
856 output_discordant.sam
857
858
859 **Visualization**
860
861 **bedtools version 2.25.0** (Quinlan & Hall 2010)
862
863 bamToBed -i sample_1_sorted.bam > sample_1_sorted.bed
864
865 genomeCoverageBed -i sample_1_sorted.bed -g 2colums.chrom.sizes -bg >
866 sample_1_sorted.bedGraph
867
868

869 **SNP calling**
870
871 **samtools + bcftools version 1.3.1** (Li 2011)
872
873 samtools mpileup -E -C50 -Q20 -q20 -uf reference.fasta sample_1_sorted.bam | bcftools call
874 --ploidy 1 -vc -O u -o sample_1.bcf
875
876 bcftools view sample_1.bcf > sample_1.vcf
877
878 bcftools filter -o sample_1_filtered.vcf -e'QUAL<20 | DP<10 | AF1<0.8' sample_1.vcf
879
880
881 **Assembly of long-read SMRT sequencing *Zymoseptoria ardabiliae* reference strain Za17**
882
883 High molecular weight DNA of the *Z. ardabiliae* strain Za17 was isolated as described in
884 (Allen et al. 2006). Single molecule real time sequencing (SMRT) was performed on a PacBio
885 RS II using 5 SMRT cells at the Functional Genomics Center Zürich, Switzerland.
886 The genome was assembled as previously described in (Plissonneau & Stürchler 2016) using
887 the assembler SMRTanalysis v 2.3.0 implemented in the Hierarchical Genome Assembly
888 Process version 3 (HGAP3) (Chin et al. 2013). Polishing was performed with Quiver that is
889 part of the SMRTanalysis suite.
890
891
892 The following commands were used for the assembly:
893
894 > source Local_SMRTanalysis/current/etc/setup.sh
895
896 > fofnTOSmrtpipeInput.py HGAP.input.fofn > HGAP.input.xml
897
898 > smrtpipe.py –D NPROC=2 –D MAX_THREADS=2 –output=Result_SMRT –
899 params=HGAP.input.xml xml:HGAP.input.xml
900
901
Assembly statistics

Z. ardabiliae (Za17)

contigs (>= 0 bp)	59
contigs (>= 1000 bp)	59
total length (bp)	38,963,581
largest contig (bp)	4,826,179
GC (%)	51.25
N50	1,413,809
N75	689,698
L50	9
L75	18

902